NASA/TM—2017–219727

Efficient Planning of Wind-Optimal Routes in North Atlantic Oceanic Airspace

Olga Rodionova
Ames Research Center, Moffett Field, California

Banavar Sridhar
Ames Research Center, Moffett Field, California

October 2017

NASA STI Program ... in Profile

Since its founding, NASA has been dedicated to the advancement of aeronautics and space science. The NASA scientific and technical information (STI) program plays a key part in helping NASA maintain this important role.

The NASA STI program operates under the auspices of the Agency Chief Information Officer. It collects, organizes, provides for archiving, and disseminates NASA's STI. The NASA STI program provides access to the NTRS Registered and its public interface, the NASA Technical Reports Server, thus providing one of the largest collections of aeronautical and space science STI in the world. Results are published in both non-NASA channels and by NASA in the NASA STI Report Series, which includes the following report types:

- TECHNICAL PUBLICATION. Reports of completed research or a major significant phase of research that present the results of NASA Programs and include extensive data or theoretical analysis. Includes compilations of significant scientific and technical data and information deemed to be of continuing reference value. NASA counterpart of peer-reviewed formal professional papers but has less stringent limitations on manuscript length and extent of graphic presentations.

- TECHNICAL MEMORANDUM. Scientific and technical findings that are preliminary or of specialized interest, e.g., quick release reports, working papers, and bibliographies that contain minimal annotation. Does not contain extensive analysis.

- CONTRACTOR REPORT. Scientific and technical findings by NASA-sponsored contractors and grantees.

- CONFERENCE PUBLICATION. Collected papers from scientific and technical conferences, symposia, seminars, or other meetings sponsored or co-sponsored by NASA.

- SPECIAL PUBLICATION. Scientific, technical, or historical information from NASA programs, projects, and missions, often concerned with subjects having substantial public interest.

- TECHNICAL TRANSLATION. English-language translations of foreign scientific and technical material pertinent to NASA's mission.

Specialized services also include organizing and publishing research results, distributing specialized research announcements and feeds, providing information desk and personal search support, and enabling data exchange services.

For more information about the NASA STI program, see the following:

- Access the NASA STI program home page at http://www.sti.nasa.gov

- E-mail your question to help@sti.nasa.gov

- Phone the NASA STI Information Desk at 757-864-9658

- Write to:
  NASA STI Information Desk
  Mail Stop 148
  NASA Langley Research Center
  Hampton, VA 23681-2199

NASA/TM—2017–219727

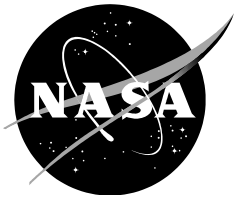

Efficient Planning of Wind-Optimal Routes in North Atlantic Oceanic Airspace

Olga Rodionova
Ames Research Center, Moffett Field, California

Banavar Sridhar
Ames Research Center, Moffett Field, California

National Aeronautics and
Space Administration

Ames Research Center
Moffett Field, CA, 94035-1000

October 2017

Acknowledgments

This research was supported by an appointment to the NASA Postdoctoral Program at NASA Ames Research Center, administrated by Universities Space Research Association through a contract with NASA. The authors would like also to gratefully acknowledge Dr. Hok K. Ng from NASA Ames Research Center for providing the data on the transatlantic flights, and Prof. Daniel Delahaye from French Civil Aviation University for his assistance in developing the optimization algorithms.

Abstract

The North Atlantic oceanic airspace (NAT) is crossed daily by more than a thousand flights, which are greatly affected by strong jet stream air currents. Several studies devoted to generating wind-optimal (WO) aircraft trajectories in the NAT demonstrated great efficiency of such an approach for individual flights. However, because of the large separation norms imposed in the NAT, previously proposed WO trajectories induce a large number of potential conflicts. Much work has been done on strategic conflict detection and resolution (CD&R) in the NAT. The work presented here extends previous methods and attempts to take advantage of the NAT traffic structure to simplify the problem and improve the results of CD&R. Four approaches are studied in this work: 1) subdividing the existing CD&R problem into sub-problems of smaller sizes, which are easier to handle; 2) more efficient data reorganization within the considered time period; 3) problem localization, i.e. concentrating the resolution effort in the most conflicted regions; 4) applying CD&R to the pre-tactical decision horizon (a couple of hours in advance). Obtained results show that these methods efficiently resolve potential conflicts at the strategic and pre-tactical levels by keeping the resulting trajectories close to the initial WO ones.

Introduction

The North Atlantic oceanic airspace (NAT) is crossed daily by more than a thousand flights cruising between North America and Europe [1]. Due to the time zone differences and passenger demands, the NAT traffic mainly contributes to the two opposite-direction flows. The majority of eastbound flights (EBFs) depart from North America in the evening and cross the NAT during the night, while westbound flights (WBFs) depart from the NAT east coast in the morning and cross the NAT in the afternoon. Thus, the traffic distribution in time is non-uniform, with two clear peaks. As a result, the airspace congestion is non-uniform in time as well reaching the maximum around 0400 UTC and 1300 UTC (all times here and after are given in UTC, Coordinated Universal Time format, displaying GMT time, where first two digits stand for hours and last two digits stand for minutes).

Another phenomenon that affects the NAT traffic is the very strong air current, jet stream [2], formed in the upper troposphere flowing from east to west. Such strong winds have an important impact on the flight progress [3-6] and thus, should be taken into account during the Flight Planning (FP) [7]. Numerous studies have been devoted to generating optimal aircraft trajectories in wind fields [8-11]; several of them are applied in the NAT [12-14]. These latter studies reveal that long-haul transatlantic flights benefit in particular from flying Wind-Optimal (WO) routes, and can achieve fuel savings of up to 10% [12]. WO routes for EBFs would follow the jet in order to take advantage from a strong tailwind, while for the WBFs, such routes would go around the jet [4]. As a result, in general, eastbound and westbound WO flows are found to be quite narrow, with high flight concentration within them; and westbound flow in general passes to the north from the eastbound flow.

Finally, an important feature that affects the Air Traffic Control (ATC) in the NAT is the lack of surveillance by radar [1]. As a result, huge horizontal (60 NM) and temporal (10 minutes) separation norms are established between aircraft in NAT in order to guarantee flight safety [15] (compared to the radar-based separation requirements of 5 NM). With the upcoming innovative surveillance and broadcast technologies [16] (such as ADS-B [17]) it is expected that these norms could be reduced by a factor of two [18-20], and several steps in this direction have already been made [21,22]. However, even being reduced to 30 NM and 3 minutes, the separation norms remain quite high. As a result, computed WO trajectories, being efficient for each individual flight [7,12], induce a large number of potential conflicts (violations of separation norms) when evaluated as an ensemble [23,24].

Conflict Detection and Resolution (CD&R) is a complex problem that has been addressed in many different ways for decades [25]. Here, mainly three types of approaches can be distinguished: tactical CD&R [26-29], performed within 30 minutes before a conflict would occur for the flights directly involved in this conflict; pre-tactical CD&R [29-31], performed up to 2 hours before a conflict occurs and

allowing more maneuver flexibility; and strategic CD&R and FP [20,32-36], performed several hours, up to several days, before the takeoff, involving all the flights planned in the airspace for the selected time period. The present paper is an extension of the previous studies [23,24,35,36] on the strategic CD&R for a large-scale airspace.

The CD&R approach developed in [35] and applied to the NAT traffic in [23,24,36] permits to formulate the CD&R problem as an optimization problem minimizing the number of potential conflicts, and then to resolve this problem using a meta-heuristic algorithm, i.e. adapted Simulated Annealing (SA), by delaying aircraft departure times and by smoothly modifying the geometric shape of aircraft trajectories. The algorithm was tested for a month of the NAT traffic, where each day involved up to 1,200 WO trajectories computed based on the flight plan restrictions and the forecast wind fields predicted for this day [12,23]. It significantly reduced the number of potential conflicts, and for the majority of cases, even eliminated them, while keeping the resulting trajectories close to the WO ones [24].

One of the advantages of the developed method is that it is quite general: it takes as an input the aircraft trajectories in terms of the sequences of route points, forecast wind fields, and established separation norms, evaluates the number of conflicts induced by this ensemble of data, and tries to reduce this number by randomly modifying (according to the SA scheme) some of the trajectories with respect to the defined modification maneuvers. Thus, the algorithm can be applied to whichever flight configuration, and not only to the NAT traffic. On the other hand, this generality makes the algorithm "blind": it does not account for any specifics of the traffic structure (such as flows directions, or flight distribution in time and space), which, in some cases, could be helpful for Conflict Resolution (CR).

The aim of the present study is to investigate how the developed method can be extended in order to take advantages of the NAT traffic features, and whether these modifications can simplify and improve CD&R in the NAT, including improving the computational efficiency of the CD&R algorithm, and improving the quality of the produced results. The paper discusses several ideas on incorporating NAT traffic particularities into the FP and CD&R procedures and is organized as follows. First, the overview of the input data used in simulations and of the previously developed CD&R algorithm is presented in Section I. Next, the algorithm modifications based on the problem decomposition are discussed in Section II. In Section III, another method, based on a simple data reorganization, is presented, which significantly decreases the problem complexity. Further in Section IV, trajectory deformations are restricted to the conflicted areas only in order to reduce the deviations from WO trajectories. Finally, in Section V, the developed strategic algorithm is adapted for pre-tactical CD&R, followed by the conclusion to this research.

Abbreviations

ADS-B	Automatic Dependent Surveillance-Broadcast
ATC	Air Traffic Control
CD	Conflict Detection
CD&R	Conflict Detection and Resolution
CR	Conflict Resolution
EBF	Eastbound Flight
FL	Flight Level
FP	Flight Planning
GFS	Global Forecast System
NAT	North Atlantic oceanic airspace
NM	Nautical Miles
NOAA	National Oceanic & Atmospheric Administration
NWP	Numerical Weather Prediction
PTCRSA	Pre-Tactical Conflict Resolution with Simulated Annealing
SA	Simulated Annealing
SCRSA	Strategic Conflict Resolution with Simulated Annealing
SCRSA/EW	Strategic Conflict Resolution with Simulated Annealing independently for Eastbound and Westbound flights
SCRSA/FL	Strategic Conflict Resolution with Simulated Annealing independently for Flight Levels
SCRSA/O	Strategic Conflict Resolution with Simulated Annealing with trajectory Optimization
SCRSA/TW	Strategic Conflict Resolution with Simulated Annealing with sliding Time Windows
SCRSAL	Strategic Conflict Resolution with Simulated Annealing with Local trajectory modifications
SCRSAL/O	Strategic Conflict Resolution with Simulated Annealing with Local trajectory modifications and trajectory Optimization
SCRSAL/TW	Strategic Conflict Resolution with Simulated Annealing with Local trajectory modifications and sliding Time Windows
TW	Time Window
UTC	Coordinated Universal Time
WBF	Westbound flight
WO	Wind-Optimal

Symbols

α, β	=	weighting coefficients for different criteria in the optimization problem
b^f	=	variable controlling the trajectory deviation of flight f
B	=	total cruising time increase related to the trajectory deviations
C_t	=	total number of point-to-point conflicts induced by a set of flights
d^f	=	delay of flight f
D	=	total delay over all flights in the flight sets
f	=	flight/trajectory index
N	=	total number of flights per day
N^f	=	number of trajectory points for flight f
q^f	=	4D trajectory point of flight f
R_{max}	=	maximal trajectory shape modification rate
W	=	an ensemble of forecast wind field for a day
z	=	vector of decision variables of the optimization problem

I. Strategic conflict detection and resolution problem formulation

This section first describes the wind and flight data for WO trajectories used in the simulations of the NAT traffic. Then, the Conflict Detection (CD) methodology, applied to record the number of conflicts for the initial WO trajectories, is presented. Next, the CR problem is formulated and the optimization algorithm used to resolve it is described. Finally, some results of the algorithm application are revealed.

A. Wind and flight data

In the present study, the simulations are performed using forecast wind data and calculated WO trajectories for the 30 days of the NAT traffic for July 2012 (from July 2nd to July 31st). Wind data are obtained from the Global Forecasting System (GFS), which is a Numerical Weather Prediction (NWP) model run by National Oceanic & Atmospheric Administration (NOAA) every 6th hour of a day. Four wind forecasts are produced daily by the GFS, for each of which corresponding *u* (east-west) and *v* (south-north) wind components are recorded in a 3-dimentional grid, covering the world airspace with 0.5° resolution in longitude and latitude, and 1,000 feet resolution in altitude. An example of forecast wind on July 15th at 0000 UTC at flight level (FL) FL370 (37,000 feet) is shown in Fig. 1 (for the *u*-component, on the top, and for the *v*-component, at the bottom). The jet stream current over the NAT can be easily distinguished from Fig. 1 (top).

For each of the 30 days, the WO trajectories are given, which are generated from the real NAT flight set data by solving the dynamic equations of aircraft motion in wind fields [12] under the constraints from the real data input parameters (origin, destination, departure time, speed, and FL). The optimization is performed under the assumption that each aircraft maintains constant airspeed (Mach number) and FL, which is often the case for a cruising phase of transatlantic flights [1]. A resulting WO trajectory is represented as a sequence of geographical points (longitude, latitude) recorded each minute from the origin airport to the destination airport (omitting takeoff and landing flight phases). It can be equally considered as a sequence of 4D-points with coordinates (longitude, latitude, altitude, time).

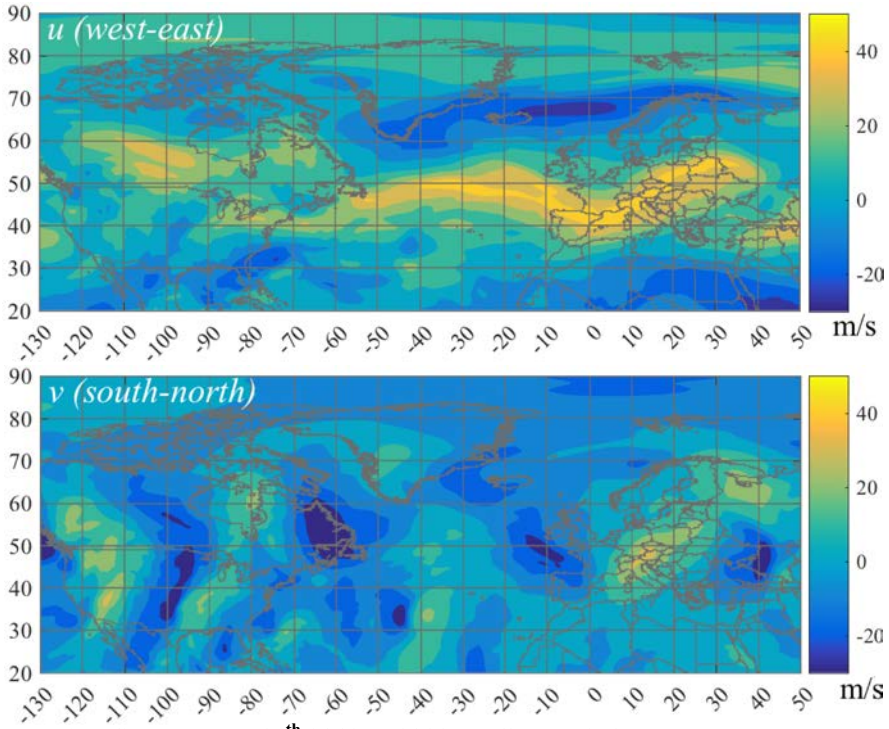

Figure 1. Forecast wind field on July 15th 2012 at 0000 UTC at FL370: *u*-component (top) and *v*-component (bottom).

In the simulations for a particular day of the NAT traffic, all the aircraft that are recorded to be in the sky on this day (from 0000 UTC to 0000 UTC on the next day) for any portion of their flight are to be considered. Among them, there are the flights departing on the current day (starting from 0000 UTC), and the flights, departed on the previous day, but landing on the current day (so-called, "transitioning flights"). Both of these flight groups contribute to the traffic (and thus, to the airspace congestion) on the current day, however, only the flights departing on the current day are subject to the strategic FP and CD&R procedures for this day. They are thus denoted as "active flights" for the current day. In contrast to them, the transitioning flights from the previous day are supposed to be planned on that previous day, and are no longer to be modified during the current day FP (on strategic level). These flights are referred as "ongoing flights" for the current day. Note that the transitioning flights are actually considered twice in the simulations for the consecutive days: first, as "active flights" on the day of their departure, and then, as "ongoing flights" on the day of their landing.

B. Conflict detection methodology

By a classical definition, a "conflict" is a violation of the established separation norms, which are to be maintained (vertically, horizontally, and, in some cases, temporally) for any two aircraft in the sky. In the present study, only conflicts detected within the NAT are considered under the reduced separation norms (as stated in the Introduction), which are established to be: 1,000 feet for vertical separation, 30 NM for horizontal separation, and 3 minutes for temporal separation (note, that a commercial aircraft cruising at the highest speed in 3 minutes would cover a distance equal to about 30 NM).

The CD method, elaborated in [35], and adapted to NAT in [23,24,36], is based on the 4-dimentional grid discretizing airspace and time, where each 4D-trajectory point is placed in an appropriate cell depending on its coordinates. The number of "point-to-point conflicts", C_t, is calculated as the number of point pairs that violate separation norms, where these pairs are taken from the same or neighbor cells of the grid. Further in this paper, however, the number of "trajectory-to-trajectory conflicts" (referred to simply as "the number of conflicts") is revealed, being a more illustrative measure. A pair of trajectories is in conflict if any pair of their points is in conflict.

Some results of the CD method application are shown in Figs. 2 and 3. For the 30 days of July 2012, there are between 1,000 and 1,200 flights crossing the NAT daily. These aircraft, when flying pre-computed WO trajectories, induce on average 400-600 potential conflicts under established separation (Fig. 2). Note, that both active and ongoing flights contribute to these numbers. In Fig. 3, an example of NAT traffic on July 15th is displayed. The two traffic flows can be clearly seen: EBFs following the jet (blue), and WBFs (black) shifted more to the north. The detected conflicts (red) are mainly situated within these flows with high flight concentration.

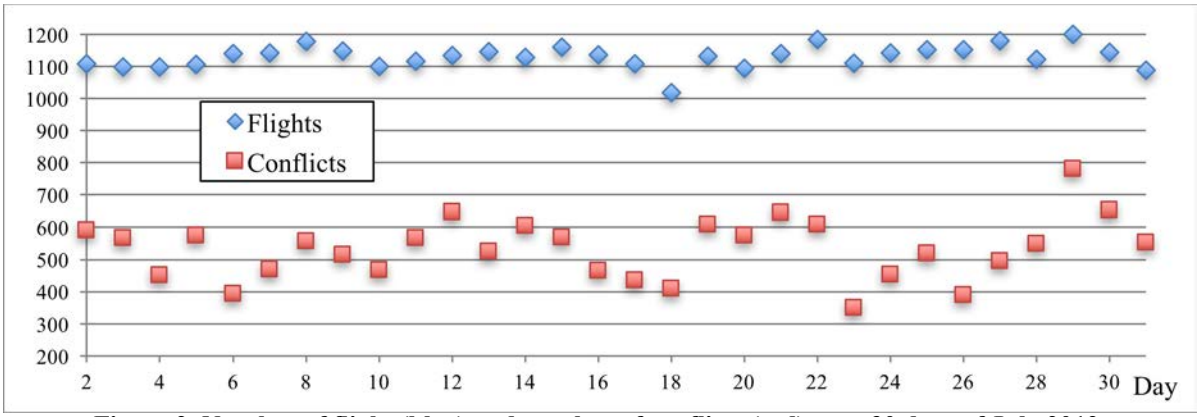

Figure 2. Number of flight (blue) and number of conflicts (red) over 30 days of July 2012.

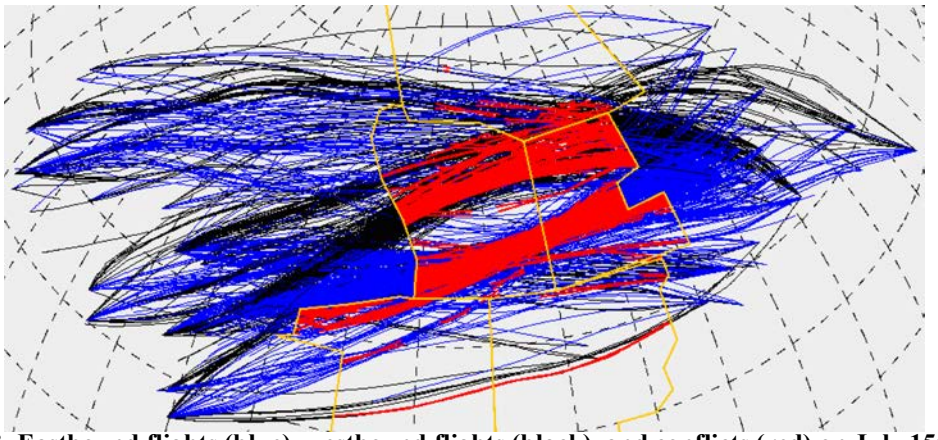

Figure 3. Eastbound flights (blue), westbound flights (black), and conflicts (red) on July 15th 2012

C. Strategic conflict resolution algorithm

The CR method for strategic FP, considered in the present study, was first developed in [35], and then adapted to NAT flights following WO trajectories in the presence of winds in [23,24,36]. First, the CR problem is formulated in terms of an optimization problem. The optimization input data for a particular day of traffic are the four wind fields for this day (for simplicity, referred further as an ensemble, W), and a set of N WO trajectories flown on this day. Each such trajectory, f ($f = 1, \dots, N$), is represented as a sequence of 4D points q_i^f ($i = 1, \dots, N^f$, where N^f is the number of points for trajectory f) in space and time.

CR requires some kind of modification of the initial trajectories. In this paper, two possible actions are considered: flight delay, and trajectory geometrical shape modification. In the first case, a random delay, d^f, is added to the given departure time of flight f. To obtain operationally acceptable results, a flight can be delayed not more than 30 minutes and by an integer number of minutes ($d^f \in \{0,1,2,\dots,30 \text{ min}\}$). In the second case, each geographical point of the given trajectory is shifted along an arc on the spherical Earth with the help of a bijection established between this trajectory and a straight-line segment [0,1] on xy-plane (Fig. 4). The straight-line segment deformation, and the corresponding shift of the trajectory points are performed using a cosine-like function. The choice of the function is conducted by the goal of keeping the resulting trajectory as smooth as the initial WO one. The function curvature is controlled independently for each flight f with a single real variable, b^f ($b^f \in [-1,1]$), which is adjusted during the optimization process; and globally for the entire flight set with a shape modification rate, R_{max}. R_{max} is a user-defined parameter which restricts the rate (in percent) of the maximum allowable length increase of the straight-line segment being deformed with the cosine-like function. Note, that the corresponding rate of the length increase of a trajectory being deformed on the spherical Earth may be greater or less than R_{max} depending on the particular trajectory position regarding the sphere curvature. More detail on the shape modification can be found in [24, 36].

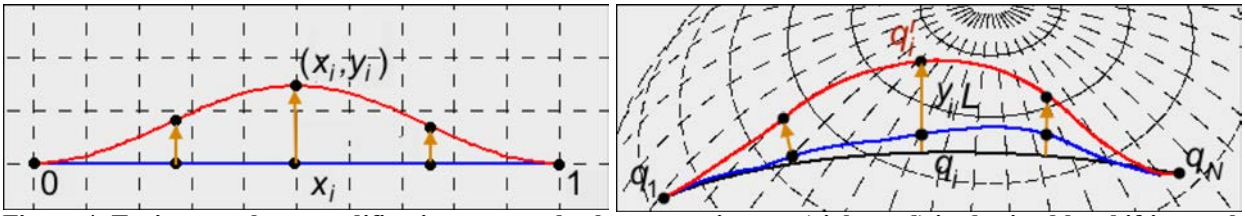

Figure 4. Trajectory shape modification approach: the new trajectory (right, red) is obtained by shifting each point q_i (from origin q_1 to destination q_N) of the initial trajectory (right, blue) along the normals (right, brown) perpendicular to the great circle (right, black) by the value y_iL, where L is the trajectory length and y_i is defined by the cosine-like funtion (left).

The values of d^f and b^f over the N flights form a vector of the optimization decision variables: $z = (d^1, b^1, \dots, d^N, b^N)$. The only optimization problem constraints are the boundary constraints on the decision variables. In the simplest formulation of the problem, presented here, the computational effort is made to conflict reduction only. The objective function to be minimized is, thus, given by the total number of point-to-point conflicts, C_t, induced by the set of modified trajectories corresponding to the variables z in the current wind conditions, W, (1):

$$\min_z C_t(z) \tag{1}$$

To obtain better solutions, additional optimization criteria, such as departure delay and flight cruising time [24], may be included into the objective function (1). The corresponding formulation is presented in Section IV.C. As the number of conflicts, C_t, cannot be explicitly expressed in terms of decision variables, z, the problem is a complex high-dimensional mixed-integer derivative-free ("black box" type) optimization problem. Thus, it was chosen to address this problem with a stochastic meta-heuristic method. The developed algorithm adapts and extends a classical Simulated Annealing (SA) algorithm [37], which arises from the thermodynamics theory of metal annealing. It is referred to in this paper as Strategic Conflict Resolution with Simulated Annealing (SCRSA).

The SCRSA is initialized with the current solution, z_0 (the given set of WO trajectories), for which the number of detected conflicts is computed. Next, two consecutive iterative processes are executed, which are traditionally referred to as "heating" and "cooling". During "heating" the "initial temperature" is calculated, which is the SA parameter needed to start the "cooling". Usually, the "heating" is performed much faster than "cooling", thus, in this paper, when comparing different versions of the SCRSA, only the number of iterations during "cooling" process is considered as the measure of the algorithm efficiency. Each such iteration involves a fixed number of evaluations. At each evaluation, the SCRSA generates a neighbor solution, z, by applying random modification maneuvers (delay or shape modification) to several appropriately chosen trajectories, and calculates the corresponding number of conflicts. The new solution is accepted or rejected according to the classical SA scheme (with some modifications aimed at improving the algorithm convergence). This step is repeated, until the conflict-free solution ($C_t = 0$) is found, or the maximum number of evaluations is achieved. In the latter case, the "initial temperature" is decreased according to the chosen SA scheme (which is known as "cooling"), and the SCRSA proceeds to the next iteration. More detail on the presented method can be found in [35,36].

D. Results of the basic conflict resolution algorithm

By applying departure time and trajectory shape modification maneuvers to the complete WO trajectories (from the origin to the destination), the SCRSA shows high efficiency in CR. For example, with the 2% shape modification rate (R_{max}=2%), the algorithm manages to resolve all the conflicts for all 30 days of July being simulated. An example of the trajectory set obtained after resolution with R_{max}=2% for July 15th is shown in Fig. 5, top. Figure 5, bottom, displays the results of the CR for the same day, but with R_{max}=1%. As it can be seen, in this latter case several conflict points still remain in the resulting solution.

There are several possible explanations to this phenomenon. First, the WO trajectory set on July 15th may be too constrained initially, and the search space given by the R_{max}=1% is not rich enough to allow conflict-free configuration. Second, the set of active trajectories on July 15th may be additionally constrained by the set of ongoing flights departed on July 14th, which is different in general for the CR with different parameters (e.g., with R_{max}). Finally, the inability to find a conflict-free flight configuration may arise from the nature of the SCRSA: as any stochastic algorithm, SA does not guarantee that the yielded solution is indeed the globally optimal one, and generally speaking, it can converge towards a local minimum.

However, the presence of a small number of conflicts in the strategic CR results is not very critical, as in any case such results are subject to uncertainties arising from different sources, including the errors in the forecast wind fields [38-40]. Due to such uncertainties, unpredicted conflicts tend to reappear when a

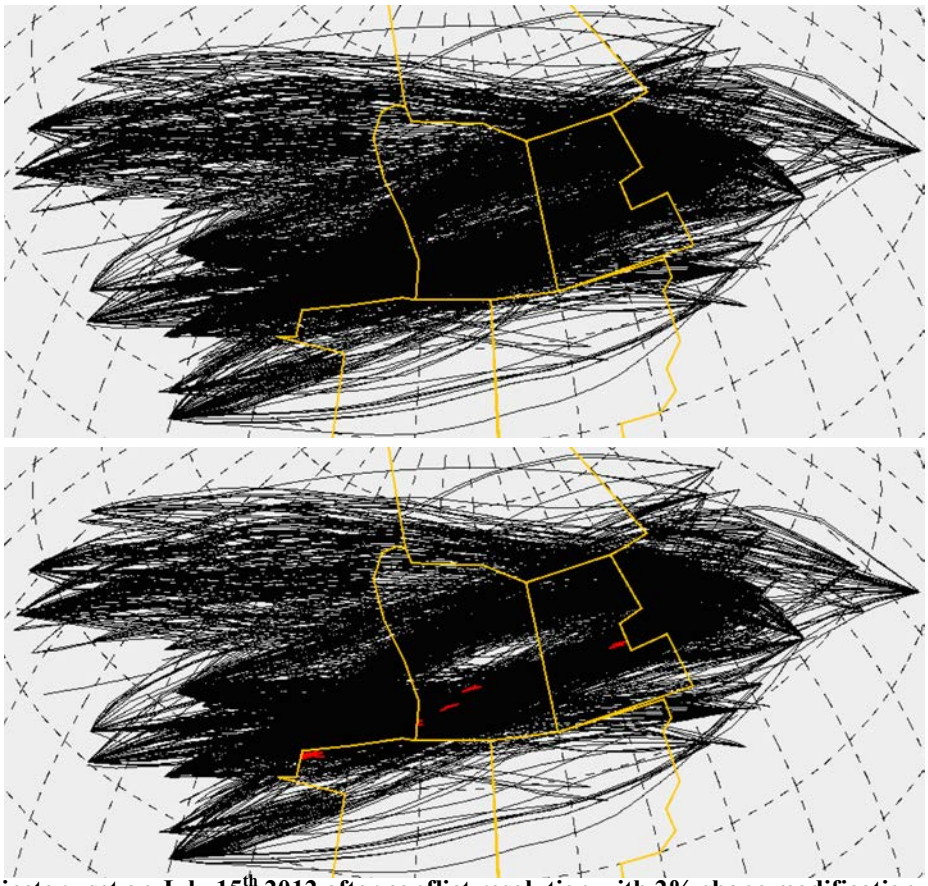

Figure 5. Trajectory set on July 15th 2012 after conflict resolution with 2% shape modification rate (top) and 1% shape modification rate (bottom) (conflict point marked with red).

conflict-free solution, yielded by the SCRSA based on the forecast wind, in evaluated over the real winds experienced by aircraft en-route (see [41] for more detail). Thus, the strategic CR gives only the preliminary results aimed at reducing the number of conflicts, and any unresolved conflicts are to be tackled during pre-tactical and tactical CR.

In addition to the efficiency of the CR, the goal of the present study is to preserve the optimality of the trajectories as far as possible. By comparing Fig. 5, top and bottom, it can be easily seen that trajectory deviations for R_{max}=1% are much smaller. Thus, such trajectories are closer to the initial WO ones. Few other comparison characteristics, averaged over the 30 days of July, for these two cases are presented in Table 1. The CR with R_{max}=1% requires, in general, more computations, as the search space is more constrained. On the other hand, as expected, it produces better results in terms of trajectory length and total cruising time increase (by almost double), and thus, better trajectory optimality. To conclude, both shape modification rates are assumed to be theoretically feasible.

Though the SCRSA seems to be quite efficient for CR, further research is needed to verify whether it can be improved when incorporating the NAT traffic features. The next section presents several methods on how the computational efficiency of the SCRSA can be addressed.

II. Improving computational efficiency by problem decomposition

One of the approaches that can potentially improve the computational efficiency of the basic algorithm, SCRSA, is to subdivide the existing CD&R problem for the whole day of NAT traffic into sub-problems of smaller size, which are easier to handle. This section proposes several ideas for such subdivision.

Table 1. Comparison of conflict resolution with different shape modification rates.

	R_{max}=2%	R_{max}=1%
Number of days with conflict remaining after CR	0	2
Total number of conflicts remaining after CR over all days	0	11
Average number of iterations to find a conflict-free solution	6.0	8.2
Average execution time to find a conflict-free solution, sec.	13.0	26.6
Mean trajectory length increase, %	0.29	0.13
Maximum trajectory length increase, %	4.8	3.3
Mean cruising time increase, %	1.11	0.63
Maximum cruising time increase, %	8.3	7.9
Percent of deviated trajectories, %	35.7	36.9
Mean delay, minutes	4.9	5.1
Percent of delayed trajectories, %	31.2	32.4

A. Flight and conflict distribution over flight levels

The first idea that comes to the mind when thinking about the problem decomposition is to treat the EBFs and WBFs independently. Indeed, they seem to be separated in time, due to the departure times, and in space, due to jet-dependent WO flows (as discussed in the Introduction); and doing so could reduce the problem by half. To validate this assumption, the number of conflicts was recorded independently for EBFs and WBFs, as well as the number of conflicts occurring between EBFs and WBFs (referred to as "mixed"). As can be seen from Fig. 6, about 15-20% of initial conflicts are of "mixed" type. This means, that EBFs and WBFs are not actually completely separated, and still interact at certain time periods.

On the other hand, when evaluating flight distribution over altitudes (Fig. 7), it can be noted, that EBFs in general occupy odd FLs (e.g. FL330, FL350, FL370), while WBFs mainly cruise on the even FLs (e.g. FL340, FL360). However, even being valid for the majority of flights, this rule does not apply to every flight (Fig. 7). It can be further observed that the wind field structure does not change significantly between the adjacent FLs, and the changes mainly affect the wind magnitude and not the direction. Figure 8 displays an example of wind fields on July 15th at 0000 UTC for the three adjacent FLs: FL350, FL360 and FL370 (as it can be seen from Fig. 7, these FLs are the most occupied ones). As a result, WO trajectories for the same origin/destination airport pairs are quite close or even identical (in horizontal profile) for the adjacent FLs. An example of such trajectories between London, Heathrow International Airport (EGLL) and New York, J.F. Kennedy International Airport (KJFK) is shown in Fig. 9 (for EBFs, on the left; and for WBFs, on the right).

The above observations give an idea that the EBFs and WBFs can be "artificially" separated by FLs: an EBF occupying an odd FL is moved up to the adjacent even FL, and a WBF cruising on the even FL is moved up to the adjacent odd FL (increasing a FL is in general more efficient than decreasing in terms of

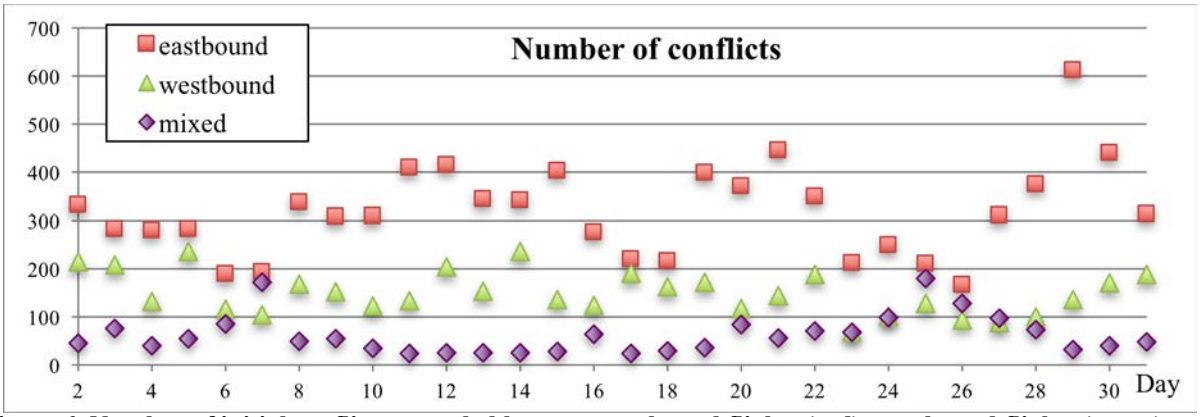

Figure 6. Number of initial conflicts recorded between eastbound flights (red), westbound flights (green), and eastbound/westbound flights (purple).

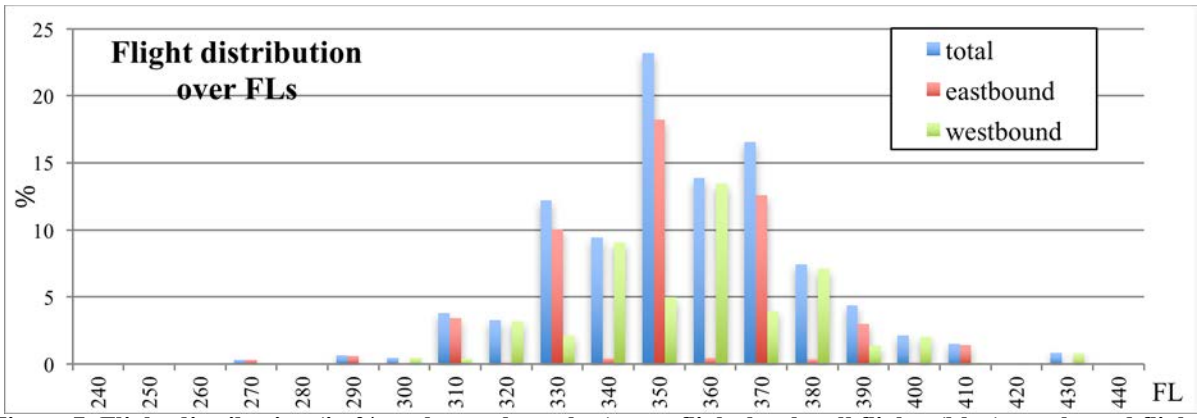

Figure 7. Flight distribution (in % to the total number) over flight levels: all flights (blue), eastbound flights (red), and westbound flights (green)

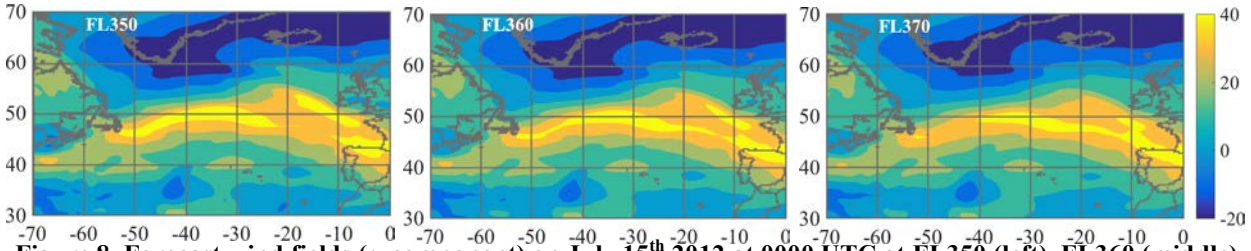

Figure 8. Forecast wind fields (*u*-component) on July 15th 2012 at 0000 UTC at FL350 (left), FL360 (middle), and FL370 (right).

Figure 9. Trajectories between London, Heathrow (EGLL) and New York, J.F. Kennedy (KJFK); 13 eastbound flights (left, black) computed with wind forcast at 0000 UTC distributed between 4 FLs (FL330, FL350, FL360, and FL370); and 9 westbound flights (right, blue) computed with wind foreacst at 1200 UTC distributed between 6 FLs (FL320, FL340, FL350, FL360, FL370, and FL380)

fuel consumption). In doing so, the opposite-direction traffic can be treated independently, as it is presented in the next section. Fig. 10, top, displays the new flight distribution over FLs obtained after the EBFs and WBFs are separated. As can be noted, it is more uniform between the FLs than for the initial data. Not surprisingly, the conflict distribution (Fig. 10, bottom) repeats the flight distribution, and is also more uniform for separated EBFs/WBFs.

As can be observed from Fig. 10, the FLs the most affected by the flight displacement are FL350, FL360 and FL370. Figure 11 presents a comparison of the number of flights occupying these FLs for the two flight sets: initial and obtained after the flight displacement. The number of flights at FL360 is significantly increased; the number of flights at FL350 is decreased noticeably, while the decrease of the number of flights at FL370 is less visible. As a result, after the displacement the flights are more evenly distributed between the most frequently used FLs. However, this fact does not improve the conflict situation for the initial WO trajectories. Indeed, though the conflicts are distributed more evenly (Fig. 10, bottom), their total number is increased by about 10%, as shown in Fig. 12, top. Figure 12 also displays the number of conflicts recorded independently for the three most frequently used FLs before and after the flight displacements. It can be noted that this number is not affected greatly for the odd (eastbound) FLs (FL350 and FL370), while the number of conflicts for the FL360 (assigned to WBFs) is significantly

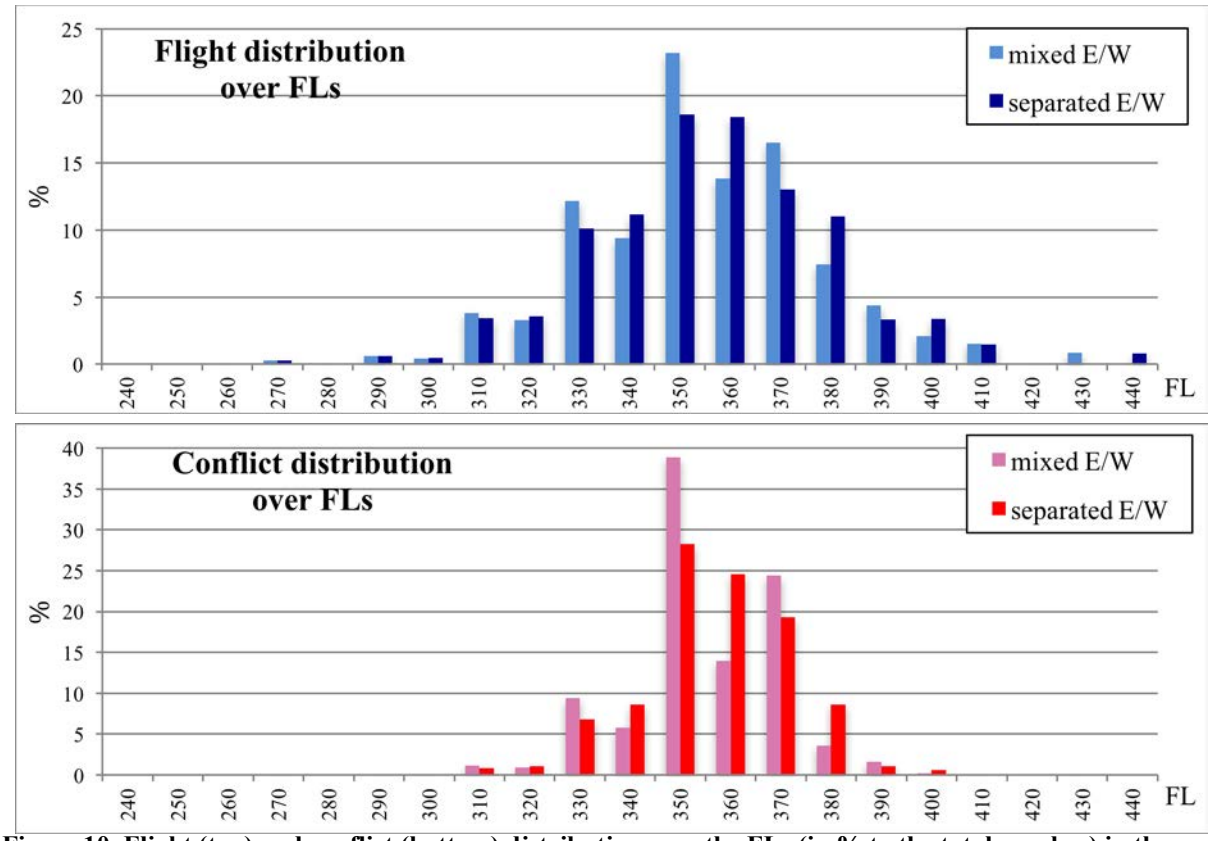

Figure 10. Flight (top) and conflict (bottom) distribution over the FLs (in % to the total number) in the case when eastbound and westbound flights may occupy the same FLs (mixed E/W) and in the case when these flights are separated (separated E/W).

increased, by almost twice on average. This could be one possible explanation to the fact why initially a non-negligible percent of WBFs occupied the adjacent odd FL.

In general, there are between 115 and 175 flights that are moved to adjacent FLs daily, which is about 15% of the total number of flights departing each day. Evidently, displacement to another FL affects the flight efficiency. However, some flights may even benefit from such a displacement in terms of the total cruising time, which can be decreased due to more favorable winds on the adjacent FL. On average, these flights constitute about 35% of the total number of affected flights. The number of flights with benefits and penalties in total cruising time due to the FL changes is shown in Fig. 13. Figure 14 displays the distribution of the number of flights over the delay (in seconds) in the total cruising time, where the negative delay means time savings. As it can be seen from Fig. 14, the majority of flights lose about 10-30 seconds on their cruise; and the maximal loss in time does not exceed two minutes for all the affected flights, which constitutes less than 1% of the total cruise duration. It is assumed that the possible fuel losses related to the FL changes are not meaningful between adjacent FLs. Thus, the possible disadvantages of such an artificial EBFs/WBFs separation are assumed to be negligible. The possible benefits are discussed in the following sections.

B. Conflict resolution separately for eastbound and westbound flights

Once the EBFs and WBFs are completely separated by different FLs, they can be treated independently, consecutively or in parallel, during the CR. In the present study, the SCRSA is adapted to perform consecutive CR for EBFs and WBFs. The algorithm is initialized and executed twice for each day and the results of both executions are merged to obtain the complete traffic situation for a day. This version of the SCRSA is further referred to as SCRSA/EW.

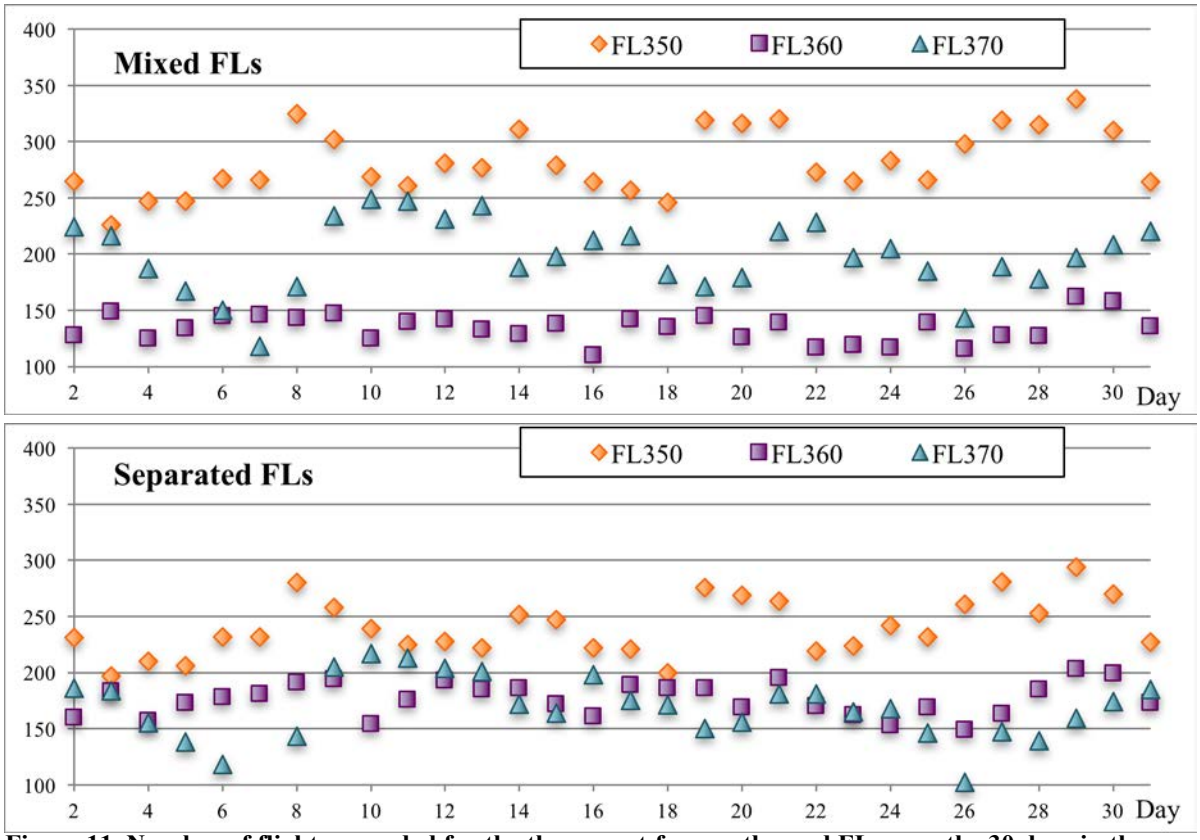

Figure 11. Number of flights recorded for the three most frequently used FLs over the 30 days in the case when eastbound and westbound flights may occupy the same FLs (top) and in the case when these flights are separated (bottom).

In order to perform a fair comparison of the SCRSA/EW and basic SCRSA, both algorithms are applied to the same data. The results presented in Section I.D were obtained for the case when EBFs and WBFs shared the FLs. The results of the SCRSA execution with 2% shape deviation rate for the case of separated FLs, discussed in this section, are summarized in Table 2. The first conclusion that can be made on comparing these results with those given in Table 1 (refer to middle columns) is that the case of separated EBFs/WBFs tends to be more difficult to resolve. Indeed, the number of iterations executed before the conflict-free solution is found, as well as the total computational time is slightly increased for this case. Moreover, there is one day, i.e. July 15th, when the algorithm failed to find a conflict-free flight set. This is surely related to the fact that the initial number of conflicts is also greater for this case (Fig. 12). In addition to this, the same issues discussed in Section I.D may affect the algorithm performance in terms of CR. The conflicts could remain due to the stochastic nature of the SA operations; or, otherwise, due to the possibility that the CR for the previous day (July 14th) produced such configurations of transitioning flights that created more constrains for the next day traffic. Indeed, the only remaining conflict is detected between an active flight and an ongoing flight. However, in terms of the trajectory optimality (including trajectory length and cruising time increase, delays, percent of delayed and deviated flights) the results for the both data sets seem to be equivalent.

The right column of Table 2 presents the results of the SCRSA/EW, executed for the same flight sets with R_{max}=2%. Here again, the conflicts remain on July 15th between the EBFs. In terms of the trajectory optimality, the results of the SCRSA/EW and SCRSA are also very similar. It seems, that on average the CR for WBFs takes a little bit more time than for the EBFs (comparing the number of iterations executed before the conflict-free solution is found); while for some specific days these are the EBFs that are constrained more. Moreover, it can be seen that each of the independent SCRSA/EW executions for EBFs and WBFs requires about half as many iterations (remind, the iterations of "cooling" process) than the SCRSA execution for the complete traffic. However, the total executional time of the SCRSA/EW is

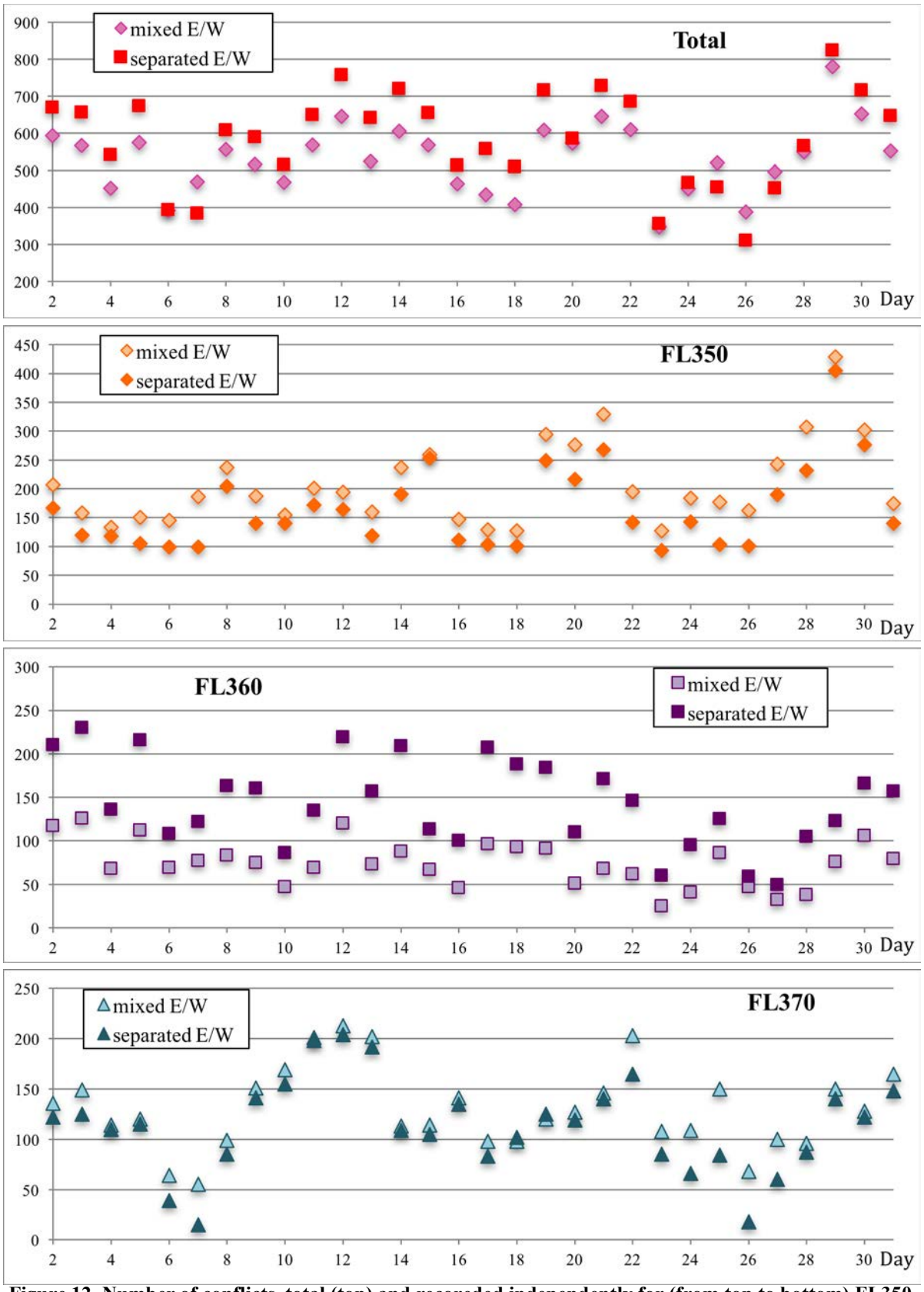

Figure 12. Number of conflicts, total (top) and recoreded independently for (from top to bottom) FL350, FL360 and FL370, over the 30 days in the case when eastbound and westbound flights may occupy the same FLs (mixed E/W) and in the case when these flights are separated (separated E/W).

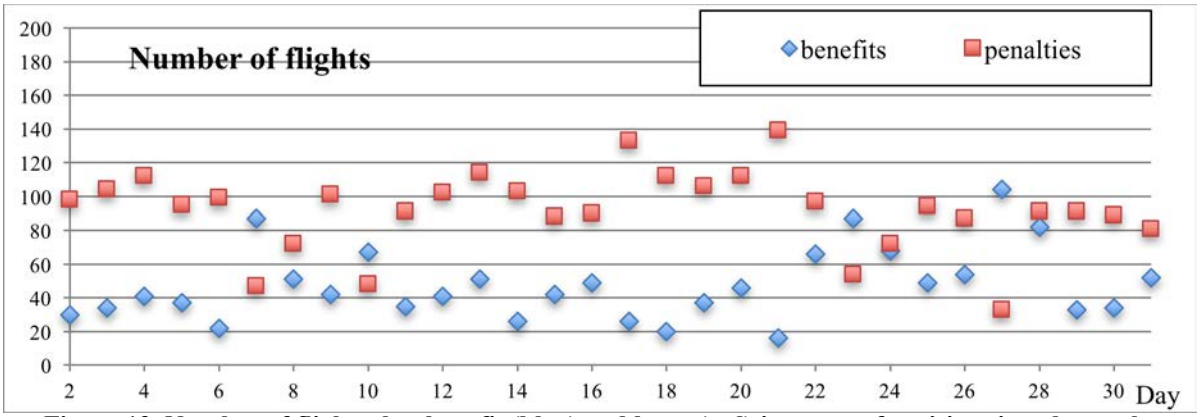

Figure 13. Number of flights that benefit (blue) and loose (red) in terms of cruising time due to the displacement to the adjacent FL.

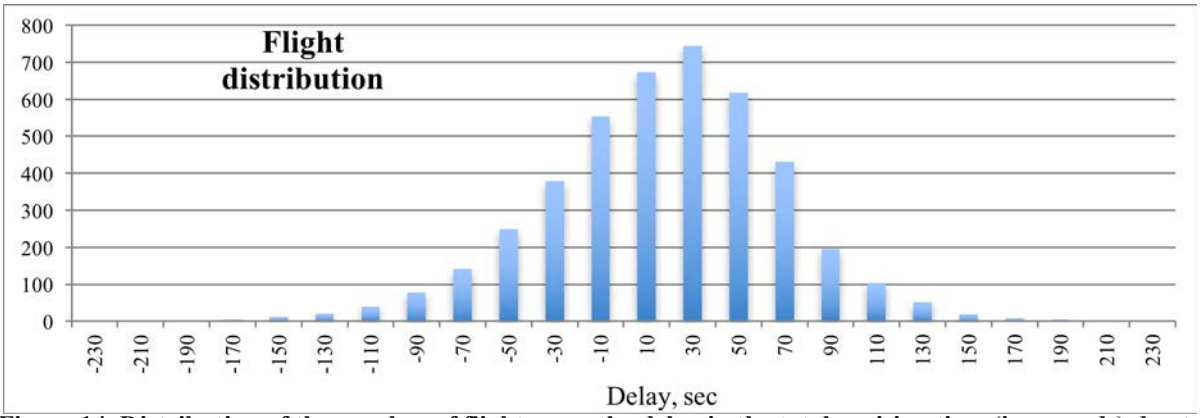

Figure 14. Distribution of the number of flights over the delay in the total cruising time (in seconds) due to the displacement to the adjacent FL (negetive delay means time savings).

about two times greater than that of the SCRSA. It can be explained by the fact that SCRSA/EW is to be initialized twice (once for eastbound and once for westbound traffic), the "heating" is to be performed twice (note, that while the "heating" is usually quite fast, it can also take some non-negligible time in particular cases), and the obtained results are to be merged in order to generate the statistics for the complete traffic. As a result, the consecutive version of the SCRSA/EW does not reveal significant benefits comparing to the SCRSA. However, as mentioned above, the processing of EBFs and WBFs can be easily parallelized, which could be promising in the conditions of the increasing traffic in the NAT.

C. Conflict resolution separately for flight levels

The next idea on how the problem complexity can be reduced is to perform CD&R separately by FLs. Indeed, for the study case, each aircraft maintains constant speed and FL from its origin to the destination. Thus, aircraft from different FLs never interact and can be considered independently. The version of the SCRSA adapted to perform consecutive CR independently for each FL is referred to as SCRSA/FL. SCRSA/FL requires initialization 21 times, which is the number of FLs available for cruise within the NAT; and then the results of the independent computations are to be merged. The simulations were performed with R_{max}=2% and for the case when the EBFs and WBFs were separated. Table 3 reveals some results of these simulations recorded independently for the three mostly occupied FLs, and for the complete set of NAT flights after merging.

The results of the SCRSA/FL are equivalent to those of the SCRSA and SCRSA/EW (Table 2) in terms of the trajectory optimality, and in terms of the number of resolved conflicts as well: the remaining conflict, occurring at FL350, is still detected for July 15th. In terms of the computational time, the CR for a

Table 2. Performance of the SCRSA and the SCRSA/EW (separated EBFs/WBFs, 2% shape modification rate).

		SCRSA	SCRSA/EW
Number of days with conflict remaining after CR		1	1
Total number of conflicts remaining after CR	over all days	1	3
	for EBFs	1	3
	for WBFs	0	0
Average number of iterations to find a conflict-free solution	total	8.5	-
	for EBFs	-	3.1
	for WBFs	-	3.7
Average execution time to find conflict-free solution, sec.		21.1	42.6
Mean trajectory length increase, %		0.28	0.27
Maximum trajectory length increase, %		4.3	4.2
Mean cruising time increase, %		1.11	1.11
Maximum cruising time increase, %		11.8	11.3
Percent of deviated trajectories, %		38.9	38.7
Mean delay, minutes		5.2	5.2
Percent of delayed trajectories, %		33.9	33.4

Table 3. Performance of the SCRSA/FL (separated EBFs/WBFs, 2% shape modification rate).

	Total	FL350	FL360	FL370
Number of days with conflict remaining after CR	1	1	0	0
Total number of conflicts remaining after CR over all days	1	1	0	0
Average number of iterations to find a conflict-free solution	-	1.7	2.8	1.4
Average execution time to find a conflict-free solution, sec.	62.3	4.4	11.2	3.0
Mean trajectory length increase, %	0.26	-	-	-
Maximum trajectory length increase, %	4.1	-	-	-
Mean cruising time increase, %	1.10	-	-	-
Maximum cruising time increase, %	14.6	-	-	-
Percent of deviated trajectories, %	38.4	-	-	-
Mean delay, minutes	5.1	-	-	-
Percent of delayed trajectories, %	33.3	-	-	-

single FL is found to be simpler than for the total flight set. For the majority of FLs, the number of aircraft and the number of conflict is so small that SCRSA/FL resolves all of them within a single iteration. For the mostly frequently used and congested FLs, i.e. FL350, FL360 and FL370, conflict-free solutions are also found much faster (in about 2-3 iterations on average) than for the total flight sets (refer to Table 2, SCRSA). However, the total computation time of the SCRSA/FL is about 1.5 times greater than that of the SCRSA/EW. It is again explained by the necessity to perform the initialization and "heating" several times; and to merge the final results. Thus, in the current conditions, consecutive CR independently for all FLs does not reduce computational time. However, similar to the SCRSA/EW, the SCRSA/FL can be simply parallelized, which could be useful in application to problems of increased traffic density.

D. Conflict resolution with sliding time windows

The next idea on how the initial problem can be subdivided into sub-problems arises from the fact that all the NAT flights are spread in time, and so are the detected conflicts. Thus, for example, a flight departing at 0100 UTC will never interact with a flight departing at 1800 UTC, and so, it is not necessary to treat them as an ensemble. To separate CR in time, a method of overlapping sliding time windows (TWs) is developed. In this case, only the flights present in NAT within a predefined TW are considered for CR. Once these flights are safely separated, the TW is shifted to overlap with the previous one. The concept of active and ongoing flights introduced to manage the consecutive-days traffic can be easily extended to the case of the consecutive TWs. The flights that entered the NAT during any previous TW

and remain in the NAT for the current TW (ongoing flights) can no longer be modified, as they were planned on the previous step; and the flights that enter the NAT during the current TW (active flights) are to avoid conflicts with the existing traffic.

The method of sliding TWs has been applied successfully for some other applications (see [42] as an example). In the present study, the extended version of the SCRSA that implements sliding TWs concept is referred to as SCRSA/TW. It was first applied to the initial data of WO trajectories in the NAT (as presented in Section I.A, where EBFs and WBFs share the FLs). The results of these simulations are presented in Table 4, middle column. The TW duration for this case was set to two hours, while the sliding shift was equal to one hour. Thus, each 2-hour TW overlaps with the previous one by one hour. The shape modification rate was again restrained to 2%.

As it can be seen from Table 4 (refer to middle column), the SCRSA/TW failed to resolve all conflicts on almost half of the days considered, for which the basic SCRSA easily found conflict-free solutions (Table 1). Investigation of these cases in detail reveals that the majority of the remaining conflicts occur between an EBF almost finishing its route, and a WBF just departing. These conflicts are, thus, due to the fact that the EBF can no longer be modified, as it was planned in one of the previous TWs, and the WBF does not have enough time and space to avoid the head conflict. However, once the EBFs and WBFs are separated by FLs, this issue is completely resolved, as can be observed from Table 4, right column. This reveals another advantage of such an EBFs/WBFs separation.

Analyzing the results produced by the SCRSA/TW for separated EBFs/WBFs (Table 4, right column) one can conclude that they are qualitatively similar to those produced by the previously discussed methods (Tables 2,3). The SCRSA/TW also failed to resolve all the conflicts for July 15th. This day seems to be indeed much more constrained than the others. In terms of the algorithm performance, the SCRSA/TW resolves conflicts easier, in general, for a single TW a smaller number of aircraft are considered within a TW. For the majority of TWs only a single iteration is performed for CR, and for some TW no CR is necessary. Table 4 displays the number of iterations needed to obtain a conflict-free solution for the three most difficult TWs, i.e. 0100-0300 UTC, 1000-1200 UTC, and 1100-1300 UTC. However, the total computational time of the SCRSA/TW is much greater than that of the SCRSA (and all its modifications discussed previously). It is also explained by the fact that the CR iterative processes are launched several times. Moreover, in the SCRSA/TW, the same flights are treated within several TWs (as long as they are present in the NAT) and thus, they are considered several times for the same day. As a result, the cumulative number of flights being treated daily is significantly increased. This was not the case for the SCRSA/EW and the SCRSA/FL, where each flight was treated just once for each day. The presented results lead to the conclusion that implementing sliding TWs does not seem to significantly improve the CR. However, this method has another important application that is discussed later.

Table 4. Performance of the SCRSA/TW (2% shape modification rate).

		Mixed E/W	Separated E/W
Number of days with conflict remaining after CR		12	1
Total number of conflicts remaining after CR over all days		20	3
Average number of iterations to find a conflict-free solution	TW 0100-0300 UTC	1.3	1.1
	TW 1000-1200 UTC	1.1	1.5
	TW 1100-1300 UTC	1.0	1.1
Average execution time to find a conflict-free solution, sec.		130.2	140.0
Mean trajectory length increase, %		0.30	0.27
Maximum trajectory length increase, %		4.4	4.2
Mean cruising time increase, %		1.09	1.08
Maximum cruising time increase, %		11.7	10.8
Percent of deviated trajectories, %		35.4	39.3
Mean delay, minutes		5.0	5.5
Percent of delayed trajectories, %		31.7	34.8

Table 5. Comparison of different extensions of the SCRSA (separated EBFs/WBFs, 1% shape modification rate).

	SCRSA	SCRSA/EW	SCRSA/FL	SCRSA/TW
Number of days with conflict remaining after CR	3	4	3	3
Total number of conflicts after CR over all days	19	10	13	14
Ave. num. of iterations to get conflict-free solution	10.6	5.5/5.4	2.5/4.0/1.6	1.3/1.9/1.5
Ave. exec. time to get conflict-free solution, sec.	42.8	80.0	91.2	160.2
Mean trajectory length increase, %	0.13	0.13	0.12	0.13
Maximum trajectory length increase, %	2.9	2.9	2.8	3.0
Mean cruising time increase, %	0.64	0.64	0.64	0.61
Maximum cruising time increase, %	7.6	8.6	5.6	8.3
Percent of deviated trajectories, %	40.1	39.8	39.6	40.2
Mean delay, minutes	5.5	5.4	5.3	5.7
Percent of delayed trajectories, %	34.8	35.0	34.3	36.2

E. Comparison of the problem decomposition methods

This section presents an additional comparison of the presented methods based on the problem decomposition into sub-problems, in order to justify the conclusions made in the previous sections. Here, the CR is performed for separated EBFs and WBFs, and with 1% shape modification rate, to see how the solution is different with smaller trajectory modifications. The obtained results are summarized in Table 5. Here, the number of iterations for the SCRSA/EW is given for EBFs/WBFs; the number of iterations for the SCRSA/FL is given for FL350/FL360/FL370; and the number of iterations for the SCRSA/TW is given for the TWs 0100-0300 UTC / 1000-1200 UTC / 1100-1300 UTC.

All the presented methods demonstrate similar efficiency in the CR, not managing to resolve conflicts for three or four days (July 15th always among them, as well as July 13th which also seems to be complicated for the CR). One can notice again that the case when EBFs and WBFs are separated by FLs is more difficult for CR (compare the number of iterations and the execution time with the results from Table 1, right column). Furthermore, the algorithms also demonstrate similar efficiency in terms of the trajectory optimality. As expected these results are about two times better in terms of trajectory length and cruising time increase than when R_{max}=2% is considered (compared to the corresponding values from Tables 2, 3 and 4). As for the delays to the departure times, their distribution is affected neither by the choice of the algorithm, nor by the choice of R_{max}.

As can be seen from Table 5, the most meaningful difference between the algorithms is observed regarding the computational time. All the versions of the SCRSA based on the problem decomposition solve each sub-problem of the CR problem in fewer iterations and less computational time, but the total computational time is higher than that of the basic SCRSA. Improving the computational efficiency can be further achieved by parallelizing the SCRSA/EW and SCRSA/FL. As for the SCRSA/TW, it cannot be parallelized, as the CR in each TW depends on the results from the previous TW. However, the possibility to treat the traffic by small portions allows expanding the range of applicability of the developed method to the pre-tactical FP and CR, as discussed in Section V.

III. Improving resolution efficiency by data reorganization

A different approach that can potentially improve the computational efficiency of the basic SCRSA algorithm arises from analyzing the results of the CR for consecutive TWs. This analysis gives an idea, of how the one-month traffic can be reorganized in order to decrease the initial problem complexity without the loss of generality. This idea is developed further in this section.

A. Flight and conflict distribution in time

From the results obtained by SCRSA/TW (Section II.D, II.E) it is noted that the most difficult resolution problems occur in the TWs at the beginning of the day, approximately from 0100 UTC to 0500 UTC. Indeed, all the remaining conflicts are detected for this particular time period. This period is characterized by the presence of non-negligible number of ongoing flights (that departed on the previous day). The CR for such flights is performed on the day of the departure; thus, for the current day, ongoing flights are considered as "hard constraints" which the active flights (departing on this current day) are to avoid. Figure 15 displays an example of the distribution of the total number of flights in the NAT (blue), as well as the number of active (red) and ongoing (green) flights, within a 24-hour time period (from 0000 UTC to 0000 UTC on the next day) for July 15th. The period when the active flights would conflict with the ongoing flights is clearly distinguished. It corresponds to the first, night-time, peak of traffic, related to the EBFs. The second traffic peak, induced by the WBFs is detected in the afternoon. Figure 16 displays the distribution of the initial number of conflicts for the given set of WO trajectories (when EBFs and WBFs share the FLs), which reflects exactly the flight distribution from Fig. 15. The ongoing flights contribute significantly to the first peak of conflicts: the majority of conflicts remaining after the CR (whichever is the CR method) occur between an ongoing flight that departed late on the previous day, and an active flight departed early on the current day, which cannot avoid by any means the ongoing flight.

On the other hand, as mentioned in the Introduction, the departure time distribution is not uniform for the NAT traffic. Figure 17 demonstrates an example of the departure time distribution within the 24-hour time period for July 15th. As it can be seen, a large number of EBFs (red) start to depart from North America around 2000 UTC. These flights cross the NAT early in the morning the next day and contribute significantly to airspace congestion within this period. At the same time, the number of departures in the

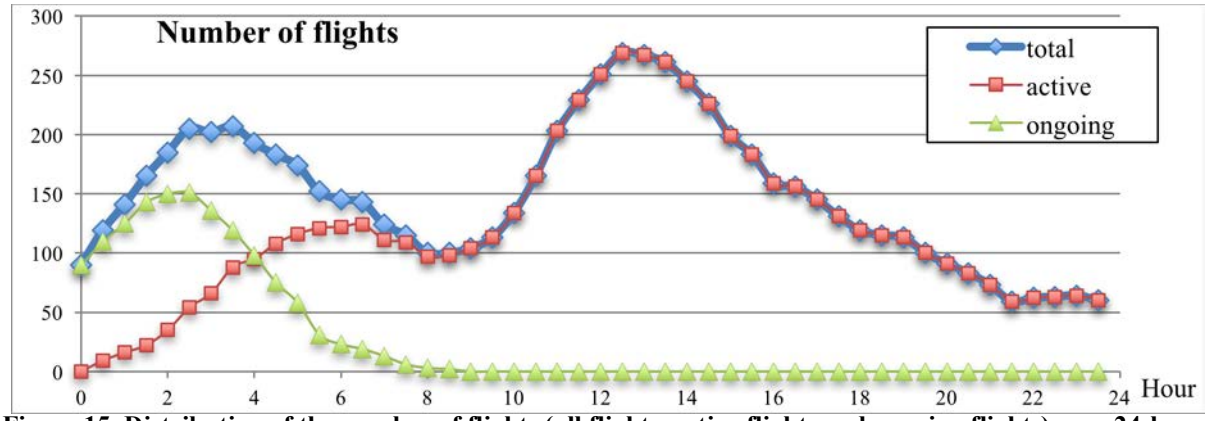

Figure 15. Distribution of the number of flights (all flights, active flights and ongoing flights) over 24-hours time period for July 15th 2012.

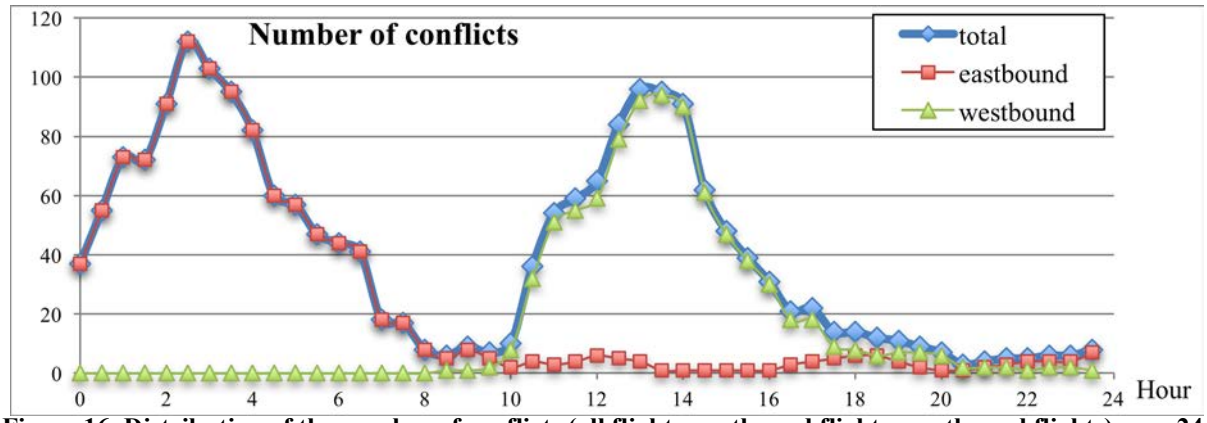

Figure 16. Distribution of the number of conflicts (all flights, eastbound flights, westbound flights) over 24-hours time period for July 15th 2012.

period just before, around 1800-1900 UTC is much smaller. In Fig. 18, the distributions of the minimum (blue), maximum (green) and average (red) values of the number of departures over the 30 days are presented. As it can be noted, the corresponding curves are very similar, thus, without loss of generality, one can consider the average value for the further analysis. In Fig. 19, this averaged distribution of the number of departures is displayed (in red) as a ratio to the maximum number of departures. In addition to this, Fig. 19 shows (in blue) the distribution of the number of flights in the NAT as a ratio to the maximum number of flights also averaged over 30 days. As it can be expected, the peaks of the NAT traffic follow the peaks of the departures with some time shift. It can be further observed that the

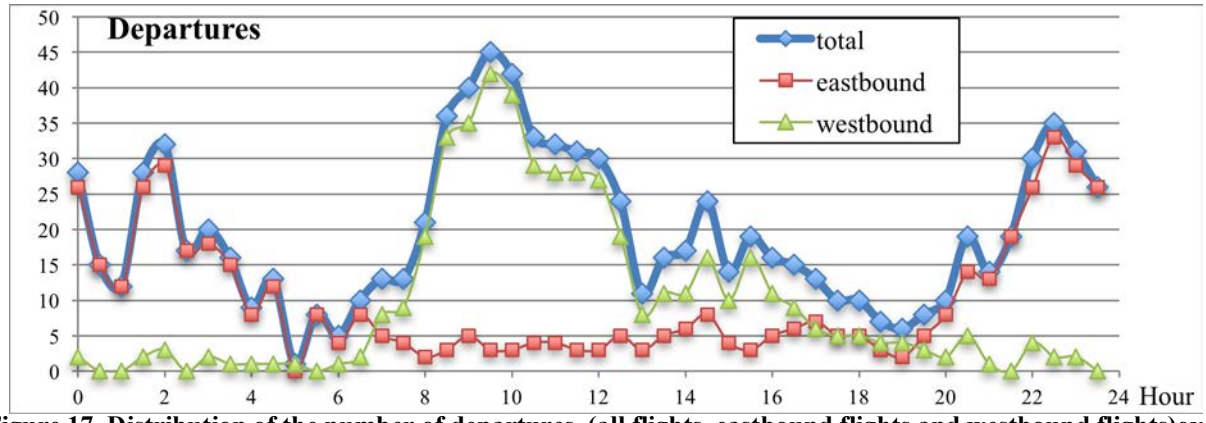

Figure 17. Distribution of the number of departures (all flights, eastbound flights and westbound flights)over 24-hours time period for July 15th 2012.

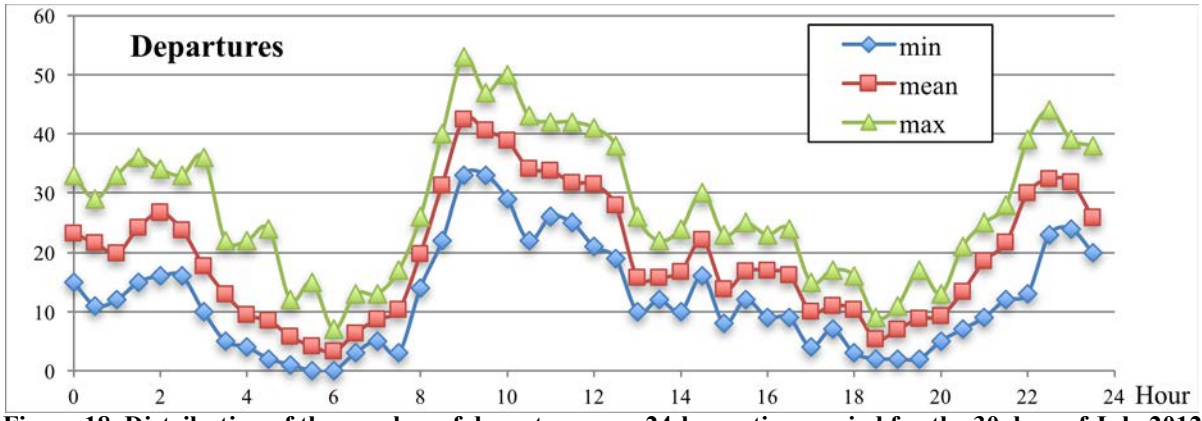

Figure 18. Distribution of the number of departure over 24-hours time period for the 30 days of July 2012 (minimum, maximum and average values).

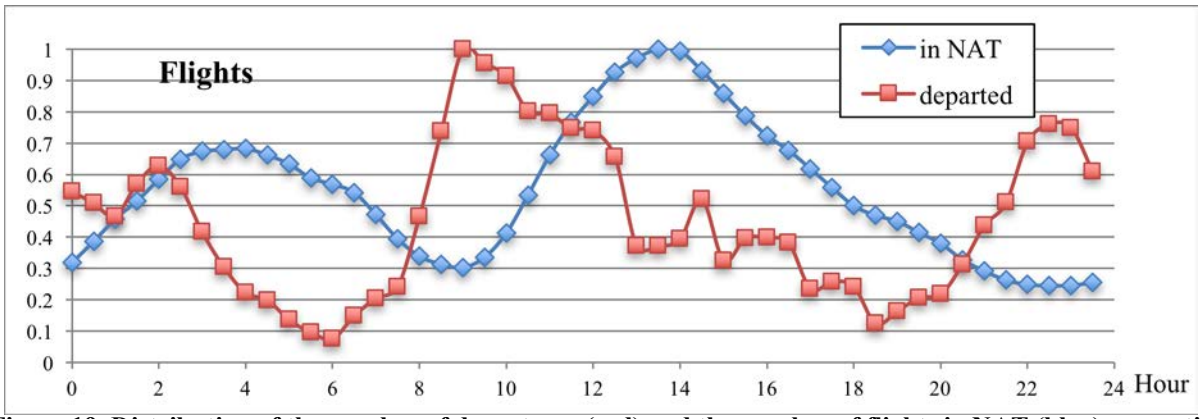

Figure 19. Distribution of the number of departures (red) and the number of flights in NAT (blue) as a ratio to the corresponding maximum numbers averaged over the 30 days within 24-hours time period.

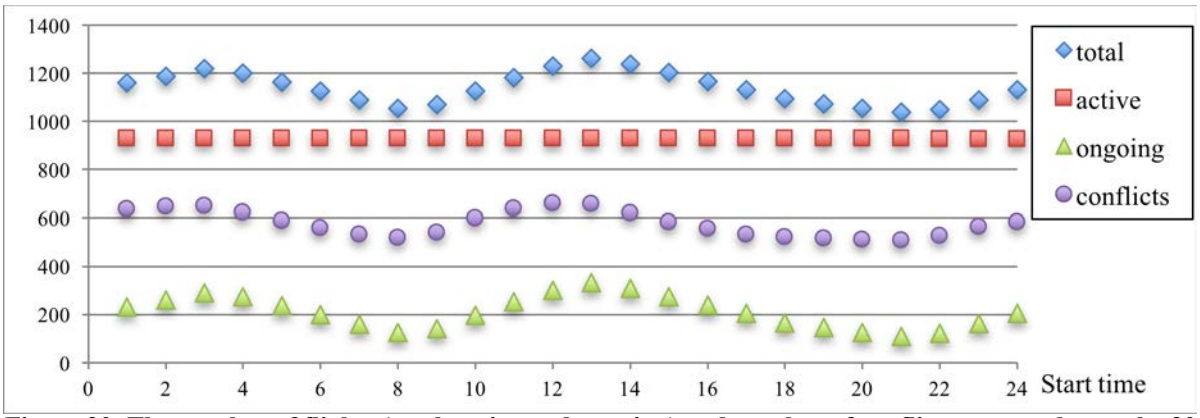

Figure 20. The number of flights (total, active and ongoing) and number of conflicts averaged over the 30 days vs the day window time shift (from 1 hour to 24 hours).

minimum of both the number of flights in the NAT and the number of departures simultaneously is achieved approximately between 2000 UTC and 2200 UTC.

The above observations give an idea that a "normal day", i.e. the period of 24 hours, from 0000 UTC to 0000 UTC on the next day, for which a set of flights is planned and conflicts are resolved, can be shifted back by several hours. For example, a 24-hours period from 2100 UTC on the previous day to 2100 UTC on the current day can be considered instead of the "normal day". The exact period does not really matter from the strategic point of view. When the FP is performed consecutively for several days (e.g. for a month), this approach does not affect the total number of flights (also for a month) being treated. On the other hand, the number of flights, which are treated for each particular day, depends on the considered 24-hours period. Figure 20 displays this dependence of the number of flights, including all flights (blue), active flights (red) and ongoing flights (green), and the number of conflicts (violet) on the day period (all values averaged over the 30 days). The *x*-axis displays the values for the "start time" of the 24-hours period. As can be noted from Fig. 20, the least number of flights per day, the least number of ongoing flights (being "hard constraints"), and the least initial number of conflicts is detected for the start time 2100 UTC, i.e. when the day period from 2100 UTC on the previous day to 2100 UTC on the current day is considered. The next section presents the results of CR for the traffic over the 30 days of July 2012 considered within these new, less restricted 24-hour time periods.

B. Conflict resolution for revised planning intervals

The CR within the shifted day interval, from 2100 UTC to 2100 UTC, was performed for the five test cases: for the case when EBFs and WBFs shared the FLs resolved by the SCRSA, and for the case when EBFs and WBFs are separated by FLs resolved be the SCRSA, the SCRSA/EW, the SCRSA/FL, and the SCRSA/TW. First, the shape modification rate was set to 1%. The corresponding results are summarized in Table 6. Again, the number of iterations for the SCRSA/EW, the SCRSA/FL, and the SCRSA/TW is given for EBFs/WBFs, for FL350/FL360/FL370; and for the TWs 0100-0300 UTC/1000-1200 UTC/1100-1300 UTC respectively. The first observation that can be made from Table 6 is the extreme efficiency of the CR for this shifted day interval. Indeed, all the conflicts are resolved for all the 30 days of NAT traffic and for all the 5 test cases. Moreover, the number of iterations and the computational time are mainly decreased comparing to the CR for the "normal day" (Tables 1 and 5). As for the results in terms of the trajectory length and cruising time increase and delays, they are comparable to those obtained previously for the "normal day".

From the above observations, it can be concluded that considering a shifted day interval is very beneficial for the CR. Moreover, as the search space with 1% shape modification rate is rich enough to permit the complete conflict elimination, one could think to reduce R_{max} in order to further restrict the trajectory deviations. Thus, the five test cases discussed above were considered for the CR with R_{max}=0.5%. The corresponding results are summarized in Table 7. As can be seen, the CR is still

Table 6. Conflict resolution within shifted day interval 2100 – 2100 UTC (1% shape modification rate).

EBFs/WBFs	Mixed	Separated			
Algorithm	SCRSA	SCRSA	SCRSA/EW	SCRSA/FL	SCRSA/TW
Number of days with conflict remaining after CR	0	0	0	0	0
Average num. of iterations conflict-free solution is found	6.2	11.0	4.2/6.9	2.4/4.3/1.7	1.5/2.1/1.5
Average exec. time conflict-free solution is found, sec.	20.3	48.5	68.9	79.2	156.1
Mean trajectory length increase, %	0.13	0.12	0.13	0.13	0.13
Max. trajectory length increase, %	2.9	3.2	3.3	2.7	2.8
Mean cruising time increase, %	0.75	0.74	0.75	0.75	0.73
Maximum cruising time increase, %	5.5	6.2	6.3	6.1	5.7
Percent of deviated trajectories, %	37.2	40.3	40.5	40.0	40.7
Mean delay, minutes	5.1	5.4	5.4	5.4	5.7
Percent of delayed trajectories, %	33.3	35.3	35.0	35.0	36.2

Table 7. Conflict resolution within shifted day interval 2100 – 2100 UTC (0.5% shape modification rate).

EBFs/WBFs	Mixed	Separated			
Algorithm	SCRSA	SCRSA	SCRSA/EW	SCRSA/FL	SCRSA/TW
Number of days with conflict remaining after CR	0	0	0	0	0
Average num. of iterations conflict-free solution is found	10.6	19.2	8.4/11.1	5.0/9.6/4.0	4.3/6.1/2.9
Average exec. time conflict-free solution is found, sec.	47.8	105.2	127.4	149.7	249.3
Mean trajectory length increase, %	0.06	0.05	0.05	0.06	0.06
Max. trajectory length increase, %	2.1	2.0	1.9	2.0	2.0
Mean cruising time increase, %	0.45	0.44	0.44	0.45	0.42
Maximum cruising time increase, %	4.8	4.7	4.2	4.6	5.7
Percent of deviated trajectories, %	38.6	41.3	41.3	41.4	41.6
Mean delay, minutes	5.3	5.7	5.7	5.6	6.0
Percent of delayed trajectories, %	34.0	36.5	36.3	36.0	37.8

extremely efficient: all conflicts are resolved. The computational time of the CR with R_{max}=0.5% is doubled (for all the methods) comparing to the CR with R_{max}=1% (Table 6), which is not surprising. On the other hand, as expected, the trajectory length and cruising time increase are about two times less in this case. One could also notice a slight increase in the number of delayed and deviated flights for the case with R_{max}=0.5%, which is due to the more constrained search space.

The examples of the resulting trajectories on July 15th obtained by the basic SCRSA for the "mixed" EBFs/WBFs for the shifted day interval are presented in Fig. 21, for 1% shape modification rate on the top, and for 0.5% shape modification rate at the bottom. The trajectory set in Fig. 21, top, looks very similar to that obtained for the "normal" day interval (Fig. 5, bottom) except, evidently, the conflict points. The trajectory set in Fig. 21, bottom, is visibly less dispersed than that on the top, and is closer to the initial WO trajectory set (Fig. 3). Using smaller shape modification rate is obviously preferable.

To conclude, it is found that a simple approach of shifting the "normal day" for strategic planning by three hours has a significant impact on the CD&R: conflicts are resolved much more easily, and with less modification maneuvers applied. Thus, this strategy is found to be very advantageous for strategic planning, and is used for further simulations.

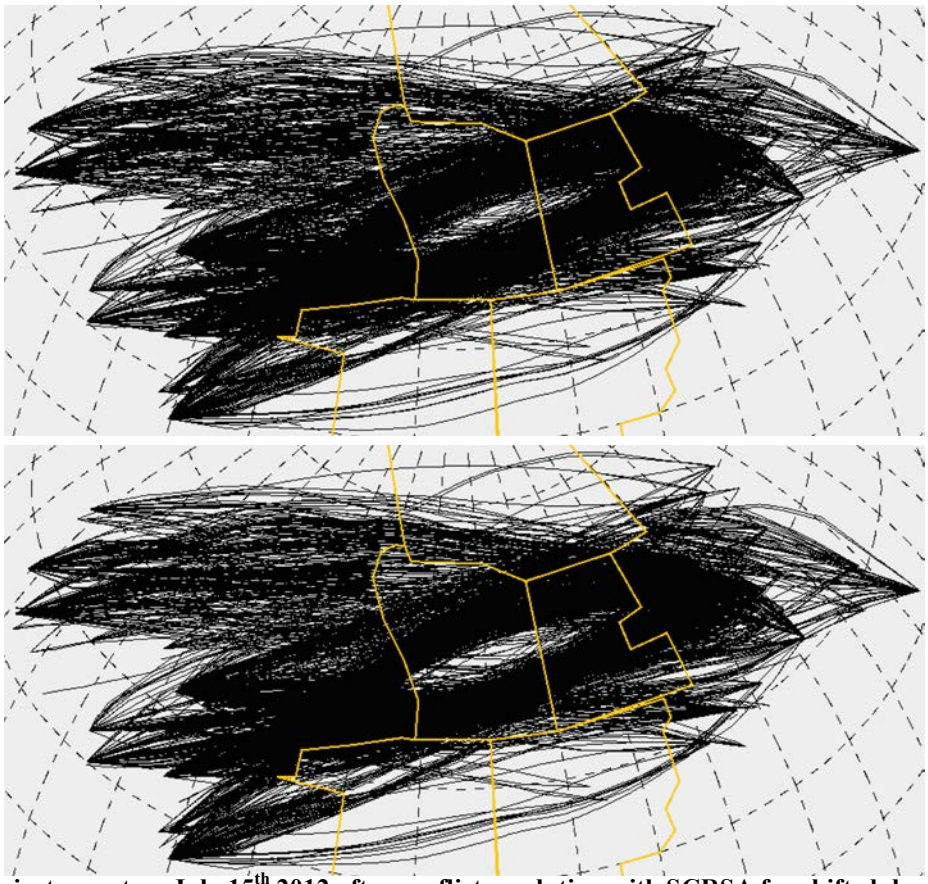

Figure 21. Trajectory set on July 15th 2012 after conflict resolution with SCRSA for shifted day interval 2100 - 2100 UTC, for 1% shape modification rate (top) and 0.5% shape modification rate (bottom).

IV. Improving resolution quality by local maneuvers

The next approach that can potentially improve the quality of the solution yielded by the basic SCRSA algorithm in terms of trajectory length and cruising time increase arises from analyzing the structure of the conflict patterns, and consists of applying local trajectory shape modifications. It is developed further in this section.

A. Local trajectory modification maneuvers

In the previous sections, the ideas for the improvement to the basic SCRSA algorithm arose from the analysis of the NAT traffic structure. In this section, the focus is shifted to the analysis of the conflict structure. Here, as described in the previous study [41], two main conflict patterns can be distinguished in NAT: "continuous conflicts", when two trajectories remain in conflict for a great portion of their length, and "spot conflicts", which happen within a very small region where the trajectories intersect. In Fig. 22, left, a trajectory from Brussels Airport (EBBR) to New York, Newark Liberty International Airport (KEWR) and a trajectory from Frankfurt Airport (EDDF) to Charlotte-Douglas International Airport (KCLT) induce a conflict of the "continuous" type; and in Fig. 22, right, a trajectory from New York, Newark Liberty International Airport (KEWR) to Oslo Gardermoen Airport (ENGM) and a trajectory from Chicago O'Hare International Airport (KORD) to Rome, Leonardo da Vinci–Fiumicino Airport (LIRF) induce a conflict of the "spot" type.

The basic SCRSA algorithm (and all its modifications described in previous sections) applies shape modification maneuvers to the complete trajectories from their origins to the destinations (Fig. 4). This CR strategy could be reasonable for "continuous" conflicts, but seems to produce unnecessary deviations

Figure 22. Examples of a "continuous conflict" (left) between trajectories from Brussels (EBBR) to New York, Liberty (KEWR) and from Frankfurt (EDDF) to Charlotte (KCLT); and a "spot conflict" (right) between trajectories from New York, Liberty (KEWR) to Oslo (ENGM) and from Chicago, O'Hare (KORD) to Rome (LIRF).

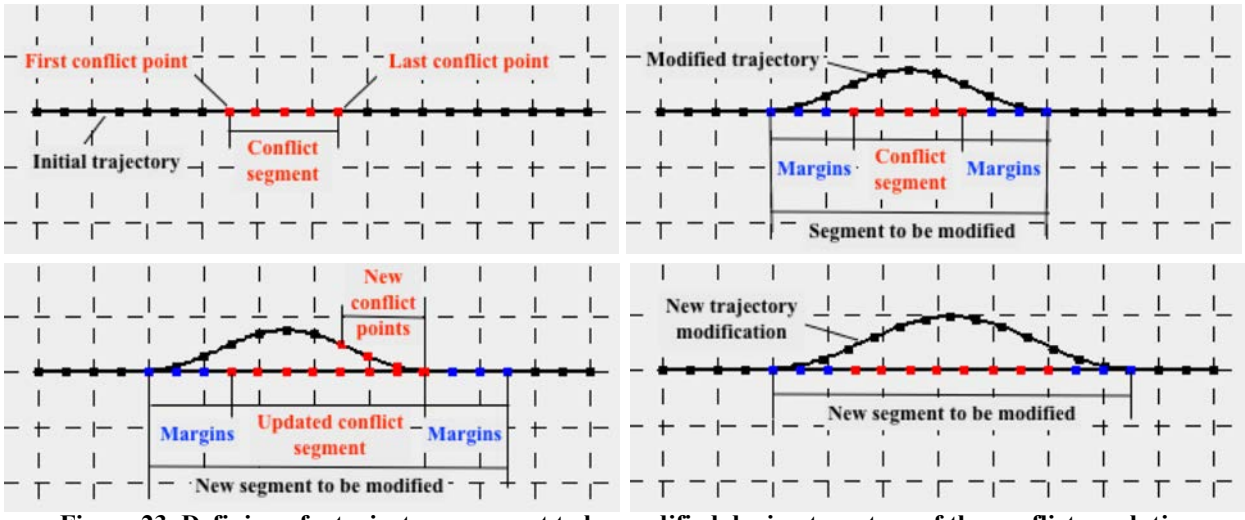

Figure 23. Defining of a trajectory segment to be modified during two steps of the conflict resolution algorithm; top, left: first step, initial trajectory and initial conflict points; top, right: first step, conflict segment with margins to be modified and the modified trajectory; bottom, left: second step, new conflict points and new trajectory segment to be modified; bottom, right: second step, new trajectory modification based on the new segment.

in the case of "spot" conflicts. Indeed, one can expect that a "spot" conflict can be avoided by just a local trajectory deformation in the vicinity of the conflict, which would result in a smaller deviation from the initial WO trajectory. Thus, in this section, such local modifications are introduced and incorporated into the SCRSA.

In order to apply local trajectory deformations one first needs to identify the trajectory segment to be modified. In this study, a simple way to define such a segment is proposed: the segment to be modified (Fig. 23, top, right) consists of a continuous sequence of trajectory points, which completely covers all the conflict points of the trajectory (Fig. 23, top, left) with some margins (Fig. 23, top, right). The margins are needed to allow enough space to avoid conflicts at the extreme points. After the initial trajectory is modified within the defined segment (Fig. 23, top, right), the new obtained trajectory is evaluated over the number of conflicts with other trajectories from the set. As a result, some new conflict points for this trajectory may be identified (Fig. 23, bottom, left). Then the segment to be modified is extended to include these new points, again with some margins (Fig. 23, bottom, left). Thus, on the next step, the trajectory modification maneuver is applied to this new extended segment (Fig. 23, bottom, right), and so on. In this approach, with the progress of the CR algorithm, the segments to be modified for each of the trajectories involved in conflicts can only increase and never decrease. However, in many cases these segments remain relatively small, which reduces the impact of the modifications on the trajectory optimality, as it will be shown in the next section.

B. Conflict resolution with local maneuvers

The simulations presented in this section were performed for the flight sets with the EBFs and WBFs separated by FLs, and for the shifted 24-hour day interval, from 2100 UTC to 2100 UTC. The benefits of such data treatment were discussed in the previous sections. The CR was performed using the basic SCRSA and SCRSA/TW extended to account for the local maneuvers. These algorithms are referred to as SCRSAL and SCRSAL/TW, where "L" stands for "local maneuvers". The conflict segment used to define the segment to be modified for a trajectory was given through the first point in conflict and the last point in conflict detected for this trajectory (Fig. 23, top, left). Each of the margins (Fig. 23, top, right) was selected to equal half of the conflict segment, but not to exceed the maximal margin size, which was adjusted in the simulations. The trajectory shape modification rate in this case was applied not to the complete trajectories, but to the trajectory segments to be modified. As in Section III, two shape modification rates were tested: R_{max}=1% and R_{max}=0.5%. For R_{max}=1%, the same maximal margin size was set in both algorithms, SCRSAL and SCRSAL/TW; while for R_{max}=0.5%, different margins sizes were used. The results of the simulations are summarized in Table 8. Again, for the methods with TWs the number of iterations is given for the TWs 0100-0300 UTC, 1000-1200 UTC and 1100-1300 UTC.

The first observation that can be made from Table 8 is that all the conflicts were completely resolved for all the studied cases. Moreover, the results of SCRSAL and SCRSAL/TW are very similar in terms of trajectory length and cruising time increases and delays (compare results of the columns 2 and 3, and 4 and 5). Thus, none of the algorithms can be distinguished as advantageous for trajectory optimality. In terms of the computational time, SCRSAL still overcomes SCRSAL/TW almost by double. It is clearly seen for R_{max}=1% (columns 2 and 3). On the other hand, in the case of R_{max}=0.5%, both algorithms seem to have equal execution time (columns 4 and 5). However, that is due to the fact that SCRSAL/TW applies larger margins and thus, has vaster search space, and converges to the minimum with more freedom.

Furthermore, one can easily notice that the parameter which affects the trajectory optimality is the shape deviation rate. On average, the trajectory length is doubled when using R_{max}=1% instead of R_{max}=0.5%, and the average cruising time increase is about 1.5 times more. The maximum length and time increases are also greater for R_{max}=1%. Thus, using a smaller shape deviation rate results in more efficient trajectories even if it may require increasing the margins in order to eliminate the conflicts. It is interesting to notice that the slight increase of the margins has almost no effect on the trajectory length and cruising time (compare columns 4 and 5, for example), while the margins length does affect the average length of

Table 8. Conflict resolution with local trajectory modification maneuvers.

Algorithm		SCRSAL	SCRSAL/TW	SCRSAL	SCRSAL/TW
Trajectory shape modification rate, %		1	1	0.5	0.5
Maximal margins size, points		60	60	72	90
Number of days with conflict after CR		0	0	0	0
Average number of iterations to find a conflict-free solution		46.7	6.5/17.7/12.5	67.0	4.6/14.7/10.7
Average execution time to find a conflict-free solution, min.		6.0	11.0	9.2	8.2
Mean trajectory length increase, %		0.08	0.08	0.04	0.04
Maximum trajectory length increase, %		2.9	2.2	1.7	1.8
Mean cruising time increase, %		0.35	0.38	0.24	0.29
Maximum cruising time increase, %		4.1	4.4	3.4	3.9
Percent of deviated trajectories, %		43.3	43.0	43.3	42.6
Mean delay, minutes		6.0	6.3	6.0	6.2
Percent of delayed trajectories, %		38.3	39.1	38.5	38.6
Length of the modified segment, in percent to the initial trajectory length	Minimum, %	2	2	2	2
	Average, %	55	63	61	74
	Maximum, %	100	100	100	100

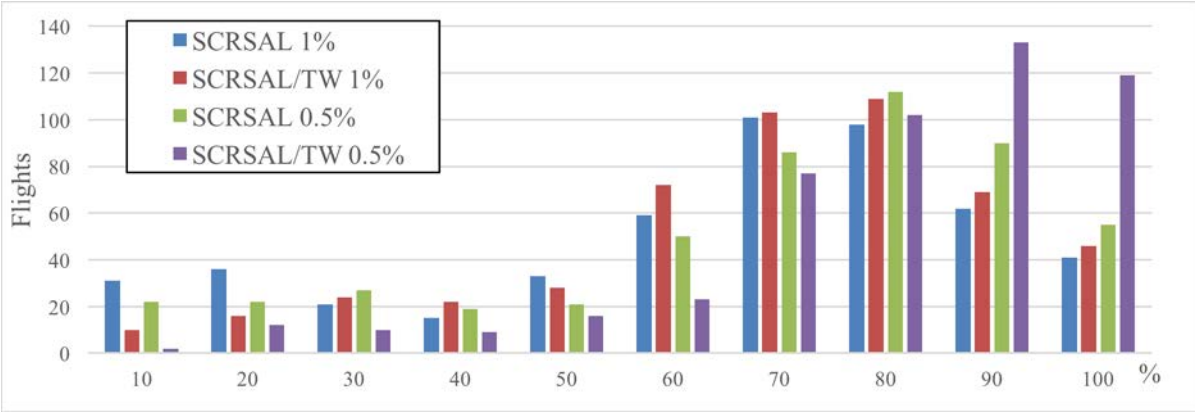

Figure 24. Distribution of the modified segment length (in % to the initial trajectory length) over all the modified flights on July 15th 2012.

the modified trajectory segments. As shown by the last three rows of Table 8, in the worst case, the modification is still applied to the complete trajectory: this is the case for the flights having their origin and destination airports just on the NAT border (e.g. a flight from New York, KJFK, to Amsterdam, EHAM). In the best case, however, only 2% of a trajectory is subject to deformation: this is the case of distant "spot" conflicts (Fig. 22, right). An example of the distribution of the segments length (in % to the initial trajectory length) for July 15th is shown in Fig. 24. It can be seen how this distribution moves towards the increase of the segments length with the increase of the margins. On average, the modified segments constitute from 50% to 70% of the initial trajectory length, and thus, it can be expected that the trajectory efficiency is better preserved in the case of local deformations compared to the complete trajectory deformations.

This last assumption is justified by comparing the results from Table 8 with those from Tables 6 and 7. The solutions yielded by the algorithms applying local trajectory modification maneuvers require noticeably less trajectory length and cruising time increases, and thus, they are closer to the initial WO trajectories. On the other hand, such solutions involve increased percentage of deviated and delayed flights (by 3% on average), and slightly increased departure delay (by half a minute on average). In Fig. 25, the solutions yielded by the SCRSAL (using R_{max}=1% on the left, and using R_{max}=0.5% on the right) for July 15th are displayed. One can see that these solutions are very similar, while it still can be noticed that the gap between EBF and WBF flows is a little bit smaller for R_{max}=1%, which is due to larger deviations applied. On comparing Fig. 25 to Fig. 21 (resolutions given by SCRSA) and Fig. 4 (initial WO trajectories), one can also visually distinguish slight improvement in the trajectory shapes corresponding to local maneuvers.

However, while the solution quality is better when applying local maneuvers, the algorithm performance remains an issue. SCRSAL (as well as SCRSAL/TW) requires significantly greater amount of computations (see Tables 6, 7, 8), which is related to the increased number of iterations due to the more restricted search space on one side, and to the increased algorithm complexity on another side. However, the computational time of 10 minutes remains reasonable for strategic FP, which is performed far in advance. Thus, the approach with local modification maneuvers can be considered to be used for the CR in the NAT. Another advantage of this approach is that it limits the trajectory deviations in the domestic airspaces, as only the trajectory segments inducing conflicts in the NAT are to be modified. Thus, it has less of an impact on the FP process. The results from Tables 6-8 are summarized in Appendix C. The next section presents some additional results of the SCRSA and SCRSAL comparison.

C. Conflict resolution with trajectory optimization

The main idea, which leads to improving the efficiency of the CR in terms of trajectory efficiency, is to reduce the trajectory deviation maneuvers and thus, to keep the resulting trajectories as close to the initial WO trajectories as possible. One of the ways to do so is to control these maneuvers during the CR, or, in

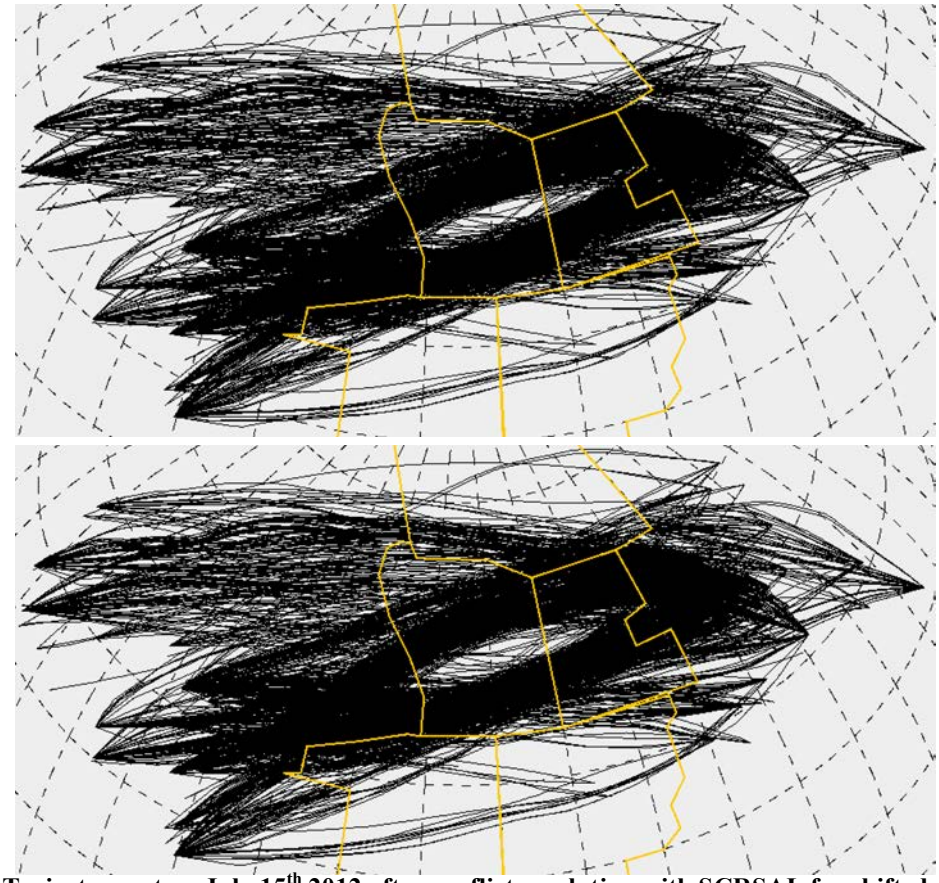

Figure 25. Trajectory set on July 15th 2012 after conflict resolution with SCRSAL for shifted day interval 2100 UTC-2100 UTC, for 1% shape modification rate (left) and 0.5% shape modification rate (right).

other words, to resolve the conflicts and to minimize the trajectory deviations simultaneously. In this case, the objective function of the optimization problem, given by (1), is to be modified in order to account for these deviations. The following objective function was used in further simulations:

$$\min_{z} C_t(z) + \alpha D(z) + \beta B(z) \tag{2}$$

Here, $C_t(z)$ is still the number of conflicts induced by the solution associated with the vector of decision variables z; $D(z)$ is the total departure delay, calculated as the sum of the delays d^f over all the N flights in the set; $B(z)$ is the total cruising time increase related to the trajectory shape modifications, also summarized over all the flights; and α and β are user-defined weighting coefficients which permit to establish the trade-off between the optimized criteria. Some more details on this method can be found in [24]. The results of the CR with the objective function (2) are presented further in this section.

The simulations were performed for the flight sets with the EBFs and WBFs separated by FLs, and for the shifted 24-hour day interval, from 2100 UTC to 2100 UTC. The CR was performed using SCRSA and SCRSAL, extended to account for trajectory deviations. Further these algorithms are referred to as SCRSA/O and SCRSAL/O (where "O" stands for "optimization"). The coefficients α and β were empirically set as following: $\beta = 1/600$, $\alpha = \beta/5$. This choice gives the highest priority to the CR criteria, which is most crucial, and the lowest priority to the departure delays, as they are considered less expensive than en-route trajectory deviations. Two shape modification rates were tested: R_{max}=1% and R_{max}=0.5%. The results of these simulations are summarized in Table 9.

Examining Table 9, one can first notice that few conflicts still remain after the CR. It seems that there are more conflicts for R_{max}=0.5% than for R_{max}=1%, and less conflicts for SCRSAL/O than for SCRSA/O. However, a definite conclusion cannot be made from these results as all the remaining conflicts are

Table 9. Conflict resolution with trajectory optimization.

Algorithm	SCRSA/O	SCRSAL/O	SCRSA/O	SCRSAL/O
Trajectory shape modification rate, %	1	1	0.5	0.5
Maximal margins size, points	-	72	-	90
Number of days with remaining conflicts	3	2	5	4
Total number of remaining conflicts	5	2	8	7
Number of iterations executed	459	459	459	459
Average executional time, minutes	24	37	27	40
Mean trajectory length increase, %	-0.08	-0.03	-0.08	-0.04
Maximum trajectory length increase, %	2.5	2.4	1.8	1.6
Mean cruising time increase, %	0.09	0.08	0.06	0.05
Maximum cruising time increase, %	4.9	3.7	2.9	2.6
Percent of deviated trajectories, %	48.4	46.8	48.9	47.6
Mean delay, minutes	3.9	4.7	4.2	4.5
Percent of delayed trajectories, %	37.5	39.9	38.7	39.5

stochastic in nature and differ from one test case to another; even the days, for which these conflicts are detected are different. Thus, the presence of the conflicts is most likely explained by the stochastic nature of the algorithm, and one can expect that by adjusting different algorithm parameters the complete resolution can be achieved. Moreover, as already mentioned in Section I.C, the presence of a small number of conflicts is not critical for strategic CR, as they are subject to uncertainties, and will be addressed at the pre-tactical and tactical stages.

In contrast to the previously discussed versions of SCRSA, the SCRSA/O and SCRSAL/O do not stop when a conflict-free solution is found ($C_t(z) = 0$) but continue the optimization in order to decrease other criteria, $D(z)$ and $B(z)$, until the maximum number of iterations is achieved. This maximum number was set equal to 459 for all the test cases. However, the total executional time is different. First of all, one can easily notice that SCRSAL/O requires about 1.5 times more computational time to fulfill the CR in comparison to SCRSA/O. That is due to the increased complexity of the algorithm when looking for the local maneuvers. Moreover, the CR with R_{max}=0.5% seems to be slightly longer than that with R_{max}=1%, which is due to the more restricted search space for the case of smaller R_{max}.

The most interesting conclusions can be made on looking to the last 7 rows of Table 9, as they reflect the resulting trajectory optimality. First of all, one can notice that the average trajectory length increase in these cases is negative, thus, the resulting trajectories tend to be more straightforward than initial WO ones. Further, it is easily seen that here again executing the algorithms with a smaller trajectory shape modification rate gives better results, especially in terms of cruising time increases (average as well as maximum). These increases are also noticeably smaller for the results of SCRSAL/O comparing to those of SCRSA/O. This observation can be explained by using the local maneuvers from one side, and by deviating fewer trajectories from another side: indeed, the percent of deviated trajectories is less for the results of SCRSAL/O. On the other hand, the percent of delayed flights, as well as the average delays assigned to these flights, are larger for the results of SCRSAL/O. This observation emphasizes the trade-off between delays and deviations when performing CR and is affected by the choice of α and β. The main result that can be formulated from Table 9 is that SCRSAL/O tends to provide better results in terms of trajectory optimality than SCRSA/O, but requires noticeably more computational time.

Some additional important conclusions can be made by comparing the results from Table 9, Table 6 (column 3), Table 7 (column 3) and Table 8 (columns 2 and 4). Obviously, the computations involving additional optimization criteria are slightly less efficient in terms of the CR, and require much more computational time (which is mainly related to the fact that the computations do not stop when a conflict-free solution is found). However, the produced results are noticeably better, especially in terms of cruising time increase, but also in terms of delays. The average delay, being about 5.5-6 minutes for SCRSA (and SCRSAL) is reduced to 4-4.5 minutes when using SCRSA/O (and SCRSAL/O), while the percent of delayed flights is not affected greatly. There is the possibility to further improve these results by adjusting accordingly the corresponding weighting coefficient (α) in the objective function. However, this

improvement can be only achieved thanks to the trade-off with trajectory optimality. In the present study, the emphasis was made to minimize the cruising time increase, and thus the corresponding coefficient β was set to be more important. More details on comparing the presented methods in terms of cruising time increase are provided in the next section.

D. Comparing of the CR methods in terms of trajectory optimality

The results concerning cruising time increase from Tables 6 (column 3), 7 (column 3), Table 8 (columns 2 and 4) and Table 9 are summarized and displayed in Fig. 26 (for average values increase on the top, and for maximum values at the bottom). One can easily see that the lowest average cruising time increase is obtained by the methods which include trajectory optimization; while the lowest maximum cruising time increase is obtained by the methods which perform local trajectory deviations. These results are not surprising, as local deviations limit the maximum length of the trajectory segments to be modified, while the CR with trajectory optimization (as it is developed in the present study) aims at minimizing the total cruising time (and not the maximum one).

In addition to this, one can observe that the improvement of the results in terms of cruising time increase is more noticeable for SCRSA/O (comparing to the SCRSA) than for the SCRSAL/O (comparing to the SCRSAL). Similarly, the improvement of the results by including the trajectory optimization in the CR is more noticeable when R_{max}=1% is used than when R_{max}=0.5% is used. To summarize, the following conclusions can be made from Fig. 26:

- The benefits brought by incorporating the cruising time increase criterion into the objective function, related with the significant increase of the computational cost, are less significant when the local maneuvers are applied than when the total trajectories are modified;

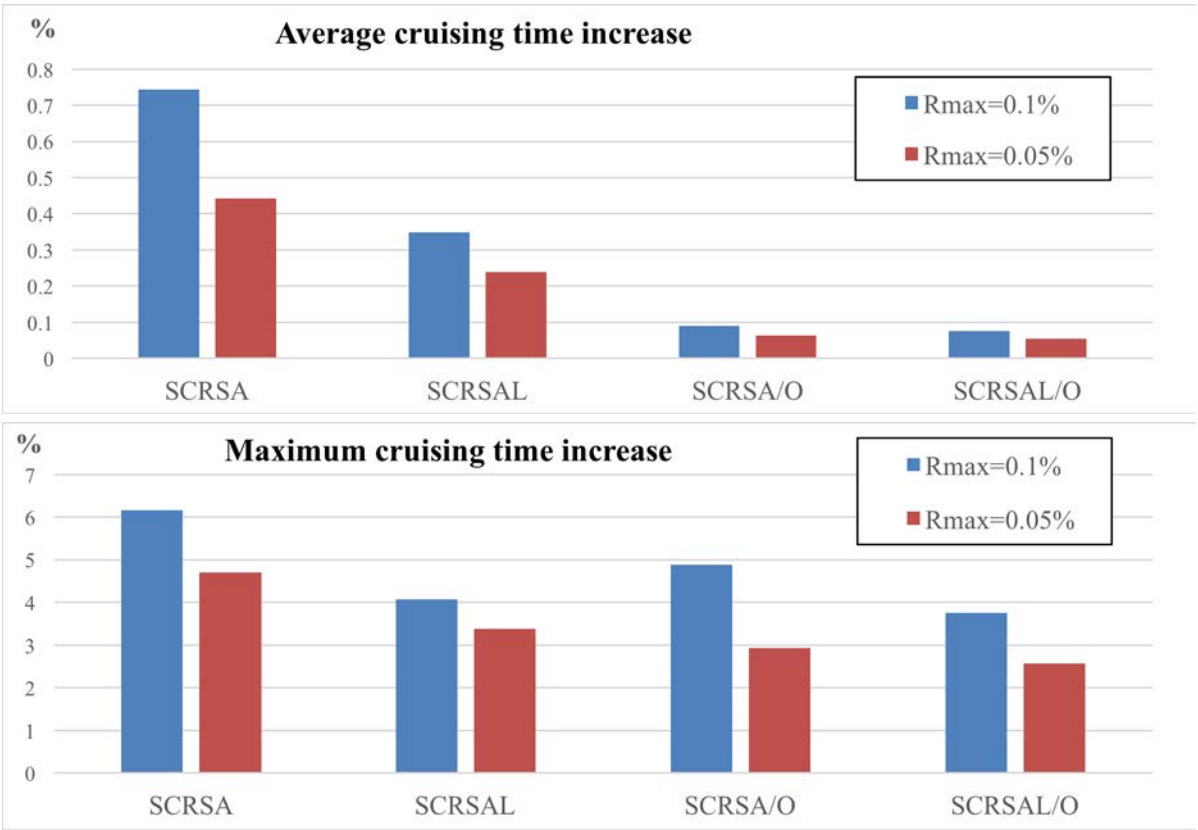

Figure 26. Comparing average (top) and maximum (bottom) cruising time increase obtained as a result of the CR with different methods.

- The benefits brought by incorporating local maneuvers, also related with the increase of the computational cost, are less significant when the trajectory optimization criteria are considered than when a simple CR is performed;
- The benefits brought by restricting the trajectory deviation with smaller shape modification rate, again related with the increase of the computational cost, are less significant when local maneuvers and/or trajectory optimization criteria are considered.

Thus, in order to choose the algorithm and the parameters most suitable for practical use, one needs to consider the trade-off between the benefits in terms of trajectory efficiency, and the penalties in terms of the algorithm complexity and computational time. The results of different strategic CR methods described above are summarized in Appendix C.

V. Pre-tactical conflict resolution

The next idea investigated in the present study explored whether the applicability of the developed strategic CD&R algorithm can be extended to cover the case of pre-tactical CD&R. Recall that the pre-tactical CD&R is performed a couple of hours in advance. That means that some conflicts may be detected and resolved before a concerned aircraft takes off, while others may only be detected between the aircraft already en-route. This section describes how the approaches presented in Section II.D for the CR with consecutive TWs and in Section IV for local trajectory deformation can be combined in order to perform pre-tactical CD&R.

A. Pre-tactical conflict resolution algorithm

Analogous to the SCRSA, the algorithm discussed in this section is referred to as PTCRSA (Pre-Tactical Conflict Resolution with Simulated Annealing). For a day of NAT traffic, the PTCRSA is executed consecutively for time periods with the duration equal to the pre-tactical time horizon. This is very similar to the concept of TWs discussed in Section II.D. To maintain the similarity, the pre-tactical time horizon was set equal to two hours, and the PRCRSA was relaunched each hour, which results in the overlapping time windows of 2-hours duration and 1-hour shift.

The PTCRSA is performed as follows. For each TW, the conflicts between the aircraft are detected only for the duration of this TW. Then, the attempt is made to resolve these conflicts by applying, similarly to the SCRSA, flight delays and/or trajectory deformations. However, the delays may only be applied to the flights which have not yet departed at the time when the PTCRSA is executed. Trajectory deformations, in their turn, can be applied to any flight, but the trajectory is restricted to be deviated only within the current TW (plus some margins). Once the CR is completed for the current TW, the obtained results are finalized. Then the PTCRSA is executed for the next TW, taking into account the results obtained from the previous step. Figure 27 displays an example of the trajectory shape modification procedure of the PTCRSA for the two consecutive TWs: TW1 with duration from t1 to t3, and TW2 with duration from t2 to t4, which overlap by the time period from t2 to t3. The trajectory is first modified during TW1 (Fig. 27, left), and the resulting trajectory becomes the initial trajectory for the next TW2 (Fig. 27, right). Note, that in Fig. 27, given as an example, the complete trajectory segment belonging to the current TW is modified. In the computational experiments, however, the segments to be modified can be also shorter as well as longer than the TW segments. More detail about this choice are given in the next section.

The PTCRSA seems to act very similarly to the SCRSAL/TW: indeed, TWs and local trajectory deformations are applied in both cases. However, there are several important differences, which arise from the nature of the CR problem at the strategic and pre-tactical levels. Looking deeper at these differences helps to understand the PTCRSA functioning. This comparison is made in Appendix A.

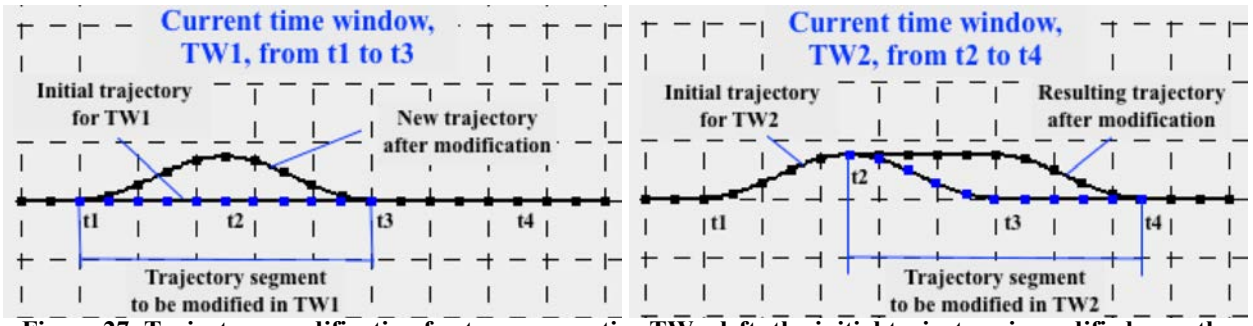

Figure 27. Trajectory modification for two consecutive TWs; left: the initial trajectory is modified over the segment belonging to the first TW; right: the trajectory, obtained withing the previous TW is modified over the segment belonging to the second TW.

B. Pre-tactical conflict resolution results

The simulations, presented in this section, were performed again for the flight sets with the EBFs and WBFs separated by FLs, and for the shifted 24-hours day interval, from 2100 UTC to 2100 UTC. First, the trajectory shape modification rate R_{max}=1% was used, as in previous sections. However, the results of the PTCRSA execution with this value turned out to be very poor, and are not included in this paper. As a consequence, the shape modification rate was increased to 5%. The results presented further were, thus, obtained with R_{max}=5%.

As discussed in Appendix A, the PTCRSA is allowed to modify a trajectory only within the current TW (with some margins). Three different strategies to define the trajectory segment to be modified within a TW were considered. For the first and second strategies, the segment to be modified was given through the first detected point in conflict and the last detected point in conflict for this trajectory (as in Fig. 23, top, left), with some margins. Each of the margins was selected to equal the length of the conflict segment, with some limitations which were different for the two strategies. In the first case, the margins were limited by the predefined maximum margin size, in a similar way as described in Section IV.B. In the presented simulations, the maximum margin size was set to be 60 trajectory points, thus, this strategy is further referred as “margins 60”. In the second case, the maximal margin size limitation was waved. This strategy is further referred as “no margins”. However, in both cases, the margin in the beginning of the segment cannot spread beyond the beginning of the current TW, as a trajectory already flown cannot be modified. Finally, for the third strategy, the trajectory segment to be modified was simply equal to the trajectory segment covered with the current TW (as in Fig. 27), with a single margin at the end of the segment (not shown in Fig. 27), which was also set to equal 60 points in the simulations. This strategy is further referred as “whole TW”. Note that the segments to be modified in the “no margins” strategy are in general greater than those in the “margins 60” strategy, and smaller than those in the “whole TW” strategy. The results of pre-tactical CR with the three described strategies are presented in Table 10.

As already mentioned above, the results of the PTCRSA with R_{max}=1% were very poor. From Table 10 it can be seen, that even when significantly greater R_{max}=5% was used, the results are not perfect: in the best case, there are still 11 days (one third of the total number of days considered) and 31 TWs for which the conflicts were not completely resolved. The remaining amount of conflicts is relatively small, i.e. less than 1% from the initial number of conflicts. Moreover, the pre-tactical CR is not the last stage, and the remaining conflicts can be further addressed during the tactical CR. However, one can easily see that the performance of the PTCRSA is much worse compared to that of the SCRSAL/TW, which seems to act very similarly. That is more likely due to the difference in the search space for both algorithms (Appendix A).

The SCRSAL/TW detects the conflicts for the complete trajectory, and thus, can apply shape modification maneuvers to longer segments, while the PTCRSA is restricted to apply these maneuvers to the current TW only. On the other hand, the PTCRSA can deform the same trajectory within several TWs (Fig. 27), which gives additional flexibility to find the conflict-free solution. Thus, most likely, the main

Table 10. Pre-tactical conflict resolution (5% shape modification rate).

Strategy for trajectory segments to be modified	"margins 60"	"no margins"	"whole TW"
Number of days with conflict remaining after CR	28	17	11
Total number of remaining conflicts	168	64	23
Average percent of resolved conflicts, %	98.9	99.6	99.9
Total number of TWs where the conflicts were not resolved (among 24 TWs and 30 days of traffic)	174	115	31
Mean trajectory length increase, %	0.62	0.62	0.82
Maximum trajectory length increase, %	7.4	6.6	11.8
Mean cruising time increase, %	0.94	0.97	1.47
Maximum cruising time increase, %	11.3	13.8	14.7
Percent of deviated trajectories, %	45.5	45.4	47.4
Mean delay, minutes	19.8	19.7	19.4
Maximum delay, minutes	59	58	56
Percent of delayed trajectories, %	13.0	12.9	11.8

difference in the algorithm performance comes from the way the departure time delay is applied. The PTCRSA cannot delay the flights that have taken off during one of the previous TWs, and this significantly limits the total number of flights which can be delayed. It can be seen from the last row of Table 10: for the PTCRSA, only 12-13% of flights received departure delays, while for the SCRSAL/TW (Table 8), this number was equal to 39%. The previous studies [24,36] already revealed that applying only the trajectory deformation maneuvers at strategic level does not provide enough flexibility to resolve all the conflicts: indeed, only about half of all conflicts were resolved in the simulations [24]. The present results for pre-tactical CR confirms this observation.

By further comparing the results from Tables 8 and 10 in terms of departure delays one can see that the delays are much greater on average for the PTCRSA: about 20 minutes against 6 minutes for the SCRSAL/TW. On one hand, that can be explained by the fact that the PTCRSA allows to delay fewer flights, and thus, each delayed flight would receive greater delay. On the other hand, that is also due to the fact that the maximum possible delay is greater for the PTCRSA. Indeed, the second row from the bottom of Table 10 shows that the maximum delays received by the flights were about one hour in this case. It could seem strange initially, as the maximum delay allowed for the CR within a single TW was still 30 minutes for the PTCRSA (as described in Section I.C). However, as the same flight can be modified within several TWs, some flights receive this delay twice. Imagine, as an example, a flight that is scheduled to depart at 0100 UTC and to enter the NAT at 0130 UTC. This flight is first considered for the CR within TW 0000-0200 UTC, some conflicts within the NAT may be detected for this flight, and as a result, it may be delayed by 30 minutes. Now it is supposed to depart at 0130 UTC and to enter the NAT at 2000 UTC. When the conflicts are resolved for the next TW, 0100-0300 UTC, the same flight can be delayed by 30 minutes in more. Thus, it will receive a total delay of 1 hour. If desired, the possibility of delaying a flight several times can be restricted in the algorithm.

Furthermore, from Table 8 it can be seen that not only the departure delay, but the trajectory length and cruising time increases are also greater for the PTCRSA, compared to those for the SCRSAL/TW from Table 8. However, the reason for this is quite obvious: the maximal shape deviation rate is 5 times greater for the simulations presented in this section. The total number of deviated flights, in its turn, is not greatly affected by the PTCRSA, and constitute about 46% against 43% for the SCRSAL/TW. The results from Tables 8 and 10 are summarized in Appendix C.

On comparing the strategies to define the trajectory segment to be deviated, one can easily see that the "margins 60" strategy is the worst in terms of conflict resolution, while the "whole TW" strategy is the best one. Thus, it seems that modifying longer segments gives more flexibility for the CR at pre-tactical level. On the other hand, the "whole TW" strategy gives the worst results in terms of trajectory optimality, which is also due to longer trajectory segments being modified; while the "margins 60" and "no margins" strategies produce very similar results. Thus, the "no margins" strategy definitively outperforms the

"margins 60". However, it is the "whole TW" strategy that was selected for farther analysis, as it was estimated that the gain in the CR exceeds the loss in trajectory optimality in this case.

In this latter case, for the absolute majority of TWs the PTCRSA manages to resolve all the conflicts in just one iteration. In several rare cases this number exceeds 30 iterations. In the worst case, 66 iterations were performed with the execution time of about 7 minutes, which remains a reasonable time for the pre-tactical CR. There are 31 TWs for which the conflicts were not completely resolved, which constitutes about 4% from the total number of times the PTCRSA was executed. These results are detailed in Appendix B. It is possible to distinguish the periods that are the most difficult for the CR, which tend to be the periods from 0200 UTC to 0600 UTC corresponding to the night traffic peak, and from 1200 UTC to 1500 UTC corresponding to the day traffic peak (Figs. 15, 16). However, the exact TWs which are the most difficult for the CR differ a lot from one day to another. This observation brings to a conclusion that the occasional inability of the PTCRSA to resolve all the conflicts is most likely related to the particular traffic structure on the particular day and within a particular TW. Indeed, it might not be physically possible to safely separate several flights having very close or even identical trajectories without the option to delay one of these flights.

Initially the results of the computational experiments performed with the PTCRSA indicate that applying the developed SCRSA to the pre-tactical problem is not very efficient. However, the inefficiency mainly comes from the limitations of the search space, and not from the limitations of the algorithm. Indeed, for the majority of the executions, at least with the "whole TW" segment modification strategy, the PTCRSA provided a conflict-free solution in just one iteration. The cases where the algorithm fails are, very probably, the cases for which the solution does not exist given the problem constraints. Thus, it can be concluded, that using the trajectory shape modifications and ground delays (applied to a small portion of flights) only is not sufficient at pre-tactical CR stage, and some additional maneuvers should be applied, such as FL and speed changes, or airborne holdings.

C. Consecutive strategic and pre-tactical conflict resolution

As it was shown in Sections I-IV, strategic CR is extremely efficient. However, as strategic conflict resolution is performed far in advance, it has to deal with estimated environmental conditions, including forecast wind fields, which may differ significantly from the real winds experienced by the aircraft en-route, and desired departure times, which may not be strictly respected for multiple different reasons. All this implies that the flight prediction at the strategic level is affected by significant uncertainties. A detailed study on the influence of the forecast uncertainties to the SCRSA results can be found in [41].

One of the results obtained in [41] indicates that when a conflict-free solution yielded by the SCRSA is evaluated in different environmental conditions, a non-negligible number of conflicts may reappear. In particular, it was found that the results of the SCRSA are robust for about 70-75% of conflicts, while about 25-30% of conflicts tend to vary with the variations of wind fields. Thus, when performing strategic CR, one can expect that the obtained results are not final, and further, when the environmental conditions are known more precisely (e.g., 2 hours before the take-off), additional CR may be needed for the reappearing conflicts. That will be the turn for the pre-tactical CR to be executed. However, its results are not final either, and the tactical CR (which is not considered in the present study) may still be needed in some cases. Taking into account all these considerations, one may ask the question whether a strategic CR makes sense.

To answer this question, a two-stage CR was imitated in the current study: the strategic CR with uncertainties followed by the pre-tactical CR. In contrast to [41], the uncertainty at the strategic level was not considered explicitly here. Instead, for each of the studied days, several flight sets were obtained from the initial flight set of WO trajectories for this day, which induced a reduced number of conflicts comparing to the initial flight set. The results presented further here are given for the flight sets inducing 5%, 25% and 50% of conflicts from the initial number of conflicts. These sets were obtained as a result of the SCRSA execution (for separated EBFs/WBFs, with R_{max}=0.5%, Section III.B), where the SCRSA was forced to stop when the desired number of reduced conflicts was achieved. For example, consider the

Table 11. Pre-tactical conflict resolution after strategic conflict resolution with different number of remaining conflicts.

Initial number of conflicts for the PTCRSA, in percent to the initial number of conflicts for WO trajectories	5%	25%	50%
Number of days with remaining conflict after the PTCRSA is executed	1	6	11
Total number of remaining conflicts after the PTCRSA is executed	1	7	18
Total number of TWs where the conflicts were not resolved (among 24 TWs and 30 days of traffic)	2	11	25
Mean trajectory length increase, %	0.74	0.77	0.80
Maximum trajectory length increase, %	11.6	9.5	9.1
Mean cruising time increase, %	1.31	1.34	1.40
Maximum cruising time increase, %	14.4	14.5	18.9
Percent of deviated trajectories, %	16.1	19.6	35.7
Mean delay, minutes	21	20.0	19.6
Percent of delayed trajectories, %	7.5	8.4	10.5

flight set obtained in this way with 5% of remaining conflicts. This flight set can also be seen as a conflict-free flight set evaluated in a slightly different environment, which results in the reappearance of 5% of the conflicts. These conflicts are then addressed at pre-tactical level, using the PTCRSA. The "whole TW" PTCRSA version with R_{max}=5% was used in these simulations. The obtained results are summarized in Table 11.

By comparing the results from Table 11 and column 4 from Table 10, one can clearly see that the lower the number of the initial conflicts for the pre-tactical stage of CR, the easier the CR is. First, fewer conflicts remain at the end of the PTCRSA execution. Second, the conflicts are not resolved for fewer TWs; and for the remaining TWs, fewer iterations are executed. Finally, fewer trajectory are deviated and delayed, and the average trajectory length and cruising time increases are also lower. Thus, the best results are obtained for the case when only 5% of conflicts remain as the input for the pre-tactical CR, which is not surprising. However, the results in the case of 25% of conflicts remaining after the strategic CR (which seems to be a realistic case taking into account varying winds [41]), are also much better than is the case when the pre-tactical CR is performed directly for the given WO trajectories. Even for the case when only 50% of conflicts are resolved at strategic level, the pre-tactical CR is still much easier and affects fewer flights. Thus, it can be concluded, that the strategic CR, even related with great uncertainties, is still advantageous and may help to reduce the workload at further levels of CR.

Conclusion

In the present study, the wind optimal (WO) trajectories in the North Atlantic oceanic airspace (NAT) were considered, and a strategic conflict resolution algorithm based on the simulated annealing metaheuristic (SCRSA) was presented. The SCRSA performs the conflict resolution (CR) simultaneously for all the flights within a 24-hour time period at the strategic level (before all flights take off) by applying two types of trajectory modification maneuvers: departure time delays and shape deformation for the complete trajectories. In the previous studies, the SCRSA had already demonstrated high efficiency by eliminating the majority of conflicts for the simulated 30 days of the NAT traffic. In this study, several modifications of the algorithm were developed and analyzed with the aim to improve the CR efficiency.

First, it was shown that the subdivision of the eastbound and westbound flights (EBFs and WBFs) into odd and even flight levels (FLs) correspondingly helps to eliminate the conflicts between the opposite-directional traffic flows. As a result, these flows can be treated separately. Several ideas of subdividing the original problem into subproblems of smaller sizes were then investigated, i.e. separate CR for EBFs and WBFs (SCRSA/EW); separate CR for FLs (SCRSA/FL); and consecutive CR for sliding overlapping time windows (TWs) (SCRSA/TW). All these modifications of the basic SCRSA produced equivalent results in terms of CR and trajectory optimality, measured mainly in terms of trajectory length and cruising time increases. The algorithm execution was indeed faster for each of the subproblems in these cases, however

the total execution times of the modified versions of the SCRSA exceed that of the basic versions. Thus, it seems, that the subdividing of the initial problem into subproblems does make sense if the parallel computations are available.

Next, the flight and conflict distributions over 24 hours of the day were analyzed, and it was found that a simple shift of the considered 24-hour time period may significantly simplify the CR. For example, on considering the flights within the time interval from 2100 UTC on the previous day to 2100 UTC on the current day (instead of the normal 0000-0000 UTC time interval), the CR is performed more efficiently and with less trajectory deformations. Several maximum trajectory shape modification rates were considered in the simulations, and it was shown that the lower this rate is, the closer the resulting trajectories are to the initial WO trajectories. On the other hand, with a decrease of the shape modification rate, the total execution time of the CR algorithm is in general increased.

Then, an attempt was made to further decrease the influence of the CR on the trajectory optimality. First, the local trajectory shape deformations (in the locality of conflict regions) were considered instead of the basic global deformations. The trajectories yielded by the CR algorithm applying local maneuvers (SCRSAL) are indeed closer to the initial WO trajectories than those obtained in previous cases. However, the execution time of the SCRSAL significantly exceeds that of the basic SCRSA. Second, the trajectory optimality criteria (total cruising time increase and total delay) were accounted for in the optimization in addition to the CR criterion. The corresponding versions of the CR algorithm (SCRSA/O and SCRSAL/O) yield very good results in terms of trajectory optimality, but they demand much more computation time. In general, the best results are produced by the algorithm which considers local trajectory deformations, trajectory optimality criteria (SCRSAL/O), and the lowest trajectory shape modification rate, but it this this combination that is the most time-consuming. Thus, one should consider a trade-off between the CR, the trajectory optimality, and the computation time.

Finally, an attempt was made to adapt the SCRSA to the pre-tactical CR (performed 2 hours in advance). The pre-tactical CR algorithm (PTCRSA) is executed consecutively for overlapping time periods (or TWs), and the results of each execution are finalized for the corresponding TW. The PTCRSA does not allow the flights which are already en-route by the time it is executed for the current TW to be delayed. Thus, for the majority of cases, only the shape deviation maneuvers are applied. The resulting search space turned out to be not rich enough to allow complete CR. As a consequence, the efficiency of the PTCRSA was lower than that of the SCRSA, and several conflicts still remained, even in the case when the shape modification rate was chosen to be quite high. However, this inefficiency is related not to the algorithm itself, but to the modification maneuvers chosen. It could be further increased by applying additional maneuvers (such as speed and/or FL changes).

The PTCRSA was then applied to evaluate the reasonability of the strategic CR. The results of these simulations demonstrated then when a certain number of conflicts is reduced at strategic level, the following pre-tactical CR is easier and more efficient. Thus, the strategic CR, even with high uncertainties, helps to decrease the airspace congestion and complexity, and the developed methods with appropriately chosen criteria and parameters help to perform the strategic CR with high efficiency.

Future research should investigate whether allowing different trajectory modification maneuvers, such as flight speed or FLs changes, in addition to departure delays and trajectory geometrical shape deformations will increase the efficiency of the strategic, and especially pre-tactical, CR. It is also possible to expand the search space of the CR with local maneuvers by introducing the variables which will define which trajectory segment should be modified instead of using conflicted segments with constant margins. Finally, the most challenging task to be addressed in the scope of the strategic CR is incorporating the environmental uncertainties into the CR. While some work in this direction has already been done for the case of wind forecast uncertainties, other uncertainty sources, in particular, possible ground delays are to be considered in order to provide the flight planning which is robust regarding potential conflicts.

Appendix A. PTCRSA vs SCRSA/TW

Although the pre-tactical CR performed with the PTCRSA looks very similar to the strategic CR with local trajectory modification maneuvers and TWs performed with the SCRSAL/TW, there are several important differences between these methods. They are summarized below.

- The PTCRSA is executed at the pre-tactical level, which means that the results of its execution for each TW are finalized and considered as the results for this time period. The SCRSAL/TW is executed at the strategic level, and the results obtained for each TW are merged at the end to obtain the new trajectory set for the whole day of traffic. For the PTCRSA, using the TWs is driven by the nature of the problem, while for the SCRSAL/TW using TWs is just a method to simplify the problem by subdividing it into sub-problems.
- Each execution of the PTCRSA should be completed at the very beginning of the TW in order to rapidly provide the flights with new trajectories if necessary. The executions of the SCRSAL/TW for all the TWs should be completed in advance, before all the aircraft take off. As a result, the SCRSAL/TW execution time is less important, and even the time of 1-2 hours is acceptable at the strategic level. In contrast, for the PTCRSA, the executional time is a crucial parameter.
- A flight is detected and considered by the PTCRSA, executed for a particular TW, as soon as it departs within this TW. It remains in the consideration for the following TWs until it exits the NAT. For the SCRSAL/TW, a flight is detected for the first time only when it enters the NAT. In other words, the flight set treated by each execution of the PTCRSA consists of flights which are present in the airspace within the current TW, while for the SCRSAL/TW, this set consists of flights present in the NAT only.
- The PTCRSA detects conflicts between the considered flights only, and within the considered TW only, and it does not consider the traffic situation for the consecutive hours. The SCRSAL/TW also detects conflicts for the considered flights only, however the detection is made for the whole length of a considered trajectory. Thus, the SCRSAL/TW also detects conflicts which would happen during future TWs. In other words, the SCRSAL/TW uses the TWs only to select the subset of flights to be considered, and the CD&R is further performed globally, for the complete trajectories. The PTCRSA, in its turn, uses the TWs not only to select the set of flights, but also to perform local CD&R.
- The PTCRSA can act with trajectory deviation maneuvers on each of the considered flights in each of the TWs. That means that a flight, which was already deviated during the PTCRSA execution for the previous TWs, may be deviated again during the current TW. In its turn, the SCRSAL/TW uses the concept of “active” and “ongoing” flights, and allows the application of trajectory deviation maneuvers to active flights only, i.e. to the flights considered for the first time during the SCRSAL/TW execution. The flights, already considered in one of the previous TWs (on-going flights), are no longer to be modified during the current TW. Using this terminology, the PTCRSA allows to modify not only active but also the ongoing flights.
- The PTCRSA and the SCRSAL/TW both apply departure time delays in order to resolve conflicts. As the SCRSAL/TW is performed at the strategic level, all of the considered “active” flights may potentially receive the delay. The PTCRSA, in its turn, is performed at pre-tactical level, and some of the flights may already be en-route when it is executed. These flights can no longer be delayed on the ground; thus, they are excluded from the set of flights to which this maneuver can be applied. Note that the flights which departed before the current TW constitute a set of “ongoing” flights for the PTCRSA. Thus, the PTCRSA applies the departure delay to “active” flights only.
- The PTCRSA and the SCRSAL/TW both apply trajectory shape modifications in order to resolve conflicts. As mentioned above, the SCRSAL/TW modifies the trajectories of “active” flights only, while the PTCRSA can apply this maneuver to all the considered flights. However, the trajectory segment which the PTCRSA is authorized to modify is limited to the considered TW only. More precisely, this segment may be extended (if necessary) by some reasonable margins to the next

TW, but not to the previous one (as, evidently, the trajectory already flown cannot be modified). For the SCRSAL/TW, the segment to be modified is defined by the conflicted areas (Figure 23), but is not limited. Thus, the SCRSAL/TW may eventually modify longer segments, but these modifications are made during a single TW only (for which the corresponding flight is active). The PTCRSA, in its turn, tends to modify considerably shorter segments during a single TW, but the modifications within several TWs are allowed, which can superpose and accumulate, so that the final deviation can be greater than that of the SCRSAL/TW (Fig. 27).

Appendix B. Performance of the PTCRSA

Table B.1 displays the total number of iterations performed by the PTCRSA using the "whole TW" strategy for each of the 24 TWs and for each of the 30 days. Each row of Table B.1 corresponds to a particular day of traffic from July 2nd to July 31st. Each column corresponds to a particular TW, from TW 2100-2300 UTC on the previous day to TW 2000-2200 UTC on the current day. The numbers in the header of Table B.1 indicate the start time for each of the TWs. Each cell of the table contains the number of iterations performed at the "cooling" stage of the algorithm before a conflict-free solution is found, or a letter "N" in case if the conflict-free solution was not found. For the majority of TWs, all the conflicts are resolved in just one iterations. In several rare cases this number exceeds 30 iterations. In the worst case, 66 iterations were performed with the execution time of about 7 minutes. There are 31 TWs for which the conflicts were not completely resolved. It is possible to visually distinguish the periods that are the most difficult for the CR: from 0200 UTC to 0600 UTC, and from 1200 UTC to 1500 UTC.

Table B.1. Number of iterations performed by the PTCRSA ("whole TW", 5% shape modification rate) to find a conflict free solution for 24 time windows and for 30 days of traffic.

	21	22	23	00	01	02	03	04	05	06	07	08	09	10	11	12	13	14	15	16	17	18	19	20
2	1	1	1	1	1	1	N	N	2	1	1	1	1	1	2	1	1	1	1	1	1	1	1	1
3	1	1	1	N	1	1	2	2	1	1	1	1	1	1	2	9	N	1	1	1	1	1	1	1
4	1	1	1	1	1	1	1	1	1	N	1	1	1	1	1	16	N	N	N	N	1	1	1	1
5	1	1	1	1	1	N	1	2	1	1	1	1	1	1	1	2	1	1	1	1	1	1	1	1
6	1	1	1	1	1	1	1	2	1	3	1	1	1	1	2	1	1	1	1	1	1	1	1	1
7	1	1	1	1	1	1	1	1	8	7	1	1	1	1	1	1	1	1	1	1	1	1	1	1
8	1	1	1	1	1	2	1	N	1	1	1	1	1	1	26	2	2	1	1	1	1	1	1	1
9	1	1	1	1	1	1	2	6	2	1	1	1	1	2	2	31	2	1	1	1	1	1	1	1
10	1	1	1	1	1	1	1	1	1	1	1	1	1	1	1	1	2	1	1	1	1	1	1	1
11	1	1	1	1	2	40	1	1	1	1	1	1	1	2	5	7	2	8	N	1	1	1	1	1
12	1	1	1	1	1	2	N	1	N	N	1	1	1	1	1	2	3	4	2	1	1	1	1	1
13	1	1	1	1	1	2	12	6	2	1	1	1	1	1	1	5	2	2	1	1	1	1	1	1
14	1	1	1	1	N	1	1	4	1	1	1	34	1	1	1	4	2	3	30	1	1	1	1	1
15	1	1	1	1	1	2	2	1	2	1	1	1	1	1	1	2	1	1	1	1	1	1	1	1
16	1	1	1	1	1	1	1	1	2	1	1	1	1	1	1	12	2	23	11	1	1	1	1	1
17	1	1	1	1	1	N	1	1	1	1	1	1	1	1	1	N	4	8	2	1	1	1	1	1
18	1	1	1	1	1	1	1	1	1	1	1	1	1	1	2	3	1	1	1	1	1	1	1	1
19	1	1	1	1	1	1	1	4	N	N	1	1	1	1	1	11	N	N	2	1	1	1	1	1
20	1	1	1	1	1	1	3	1	7	1	1	1	1	1	1	1	1	1	1	1	1	1	1	1
21	1	1	N	1	1	1	3	N	N	1	1	1	1	1	1	3	66	2	1	1	1	1	1	1
22	1	1	1	1	2	N	1	1	1	5	1	1	1	1	1	1	2	1	1	1	1	1	1	1
23	1	1	1	1	1	22	1	1	1	1	1	1	1	1	1	2	1	1	1	1	1	1	1	1
24	1	1	1	1	1	1	1	1	1	1	3	1	1	1	1	1	2	2	1	1	1	1	1	1
25	1	1	1	1	1	1	1	1	1	1	1	1	1	1	1	1	1	1	1	1	1	1	1	1
26	1	1	1	1	1	1	1	N	1	1	1	1	1	1	1	1	2	1	1	1	1	1	1	1
27	1	1	1	1	1	1	1	1	1	N	1	1	1	1	1	1	1	1	1	1	1	1	1	1
28	1	1	1	1	1	1	1	1	1	2	1	1	1	1	1	1	1	1	1	1	1	1	1	1
29	1	1	1	1	2	2	9	N	N	21	1	1	1	1	2	8	2	1	1	1	1	1	1	1
30	1	1	1	1	2	5	1	1	N	1	1	1	1	1	1	4	2	2	1	1	1	1	1	1
31	1	1	1	1	1	2	3	1	1	1	1	1	1	1	1	2	1	1	1	1	1	1	1	1

Appendix C. Conflict resolution methods summary

Table C.1 summarizes the results from Tables 6-10 for all CR methods discussed in this paper. These results are given for the simulations performed for the case when eastbound and westbound traffic flows are separated by FLs and for the shifted time period 2100-2100 UTC.

Table C.1. Conflict resolution results (separated EBFs/WBFs, shifted day interval 2100-2100 UTC).

Algorithm	Traj. Shape modification rate, R_{max}	Num. of days with conflict remaining after CR	Total num. of confl. remain. after CR over all days	Ave. num. of iterations to find a confl.-free solution	Ave. exec. time to find a conflict-free solution, sec.	Mean traj. len. incr., %	Max. traj. len. incr., %	Mean cruising time incr., %	Max. cruising time incr., %	% of deviated trajectories	Mean delay, minutes	% of delayed trajectories
SCRSA	1%	0	0	11.0	49	0.12	3.2	0.74	6.2	40.3	5.4	35.3
	0.5%	0	0	19.2	105	0.05	2.0	0.44	4.7	41.3	5.7	36.5
SCRSA/EW	1%	0	0	4.2/6.9	69	0.13	3.3	0.75	6.3	40.5	5.4	35.0
	0.5%	0	0	8.4/11.1	127	0.05	1.9	0.44	4.2	41.3	5.7	36.3
SCRSA/FL	1%	0	0	2.4/4.3/1.7	79	0.13	2.7	0.75	6.1	40.0	5.4	35.0
	0.5%	0	0	5.0/9.6/4.0	150	0.06	2.0	0.45	4.6	41.4	5.6	36.0
SCRSA/TW	1%	0	0	1.5/2.1/1.5	156	0.13	2.8	0.73	5.7	40.7	5.7	36.2
	0.5%	0	0	4.3/6.1/2.9	249	0.06	2.0	0.42	5.7	41.6	6.0	37.8
SCRSAL margins 60	1%	0	0	46.7	360	0.08	2.9	0.35	4.1	43.3	6.0	38.3
	0.5%	0	0	67.0	552	0.04	1.7	0.24	3.4	43.3	6.0	38.5
SCRSAL/TW margins: 72	1%	0	0	6.5/17.7/12.5	660	0.08	2.2	0.38	4.4	43.0	6.3	39.1
SCRSAL/TW margins: 90	0.5%	0	0	4.6/14.7/10.7	492	0.04	1.8	0.29	3.9	42.6	6.2	38.6
SCRSAL/O	1%	3	5	-	1440	-0.08	2.5	0.09	4.9	48.4	3.9	37.5
	0.5%	5	8	-	1620	-0.08	1.8	0.06	2.9	48.9	4.2	38.7
SCRSAL/O margins: 72	1%	2	2	-	2220	-0.03	2.4	0.08	3.7	46.8	4.7	39.9
SCRSAL/O margins: 90	0.5%	4	7	-	2400	-0.04	1.6	0.05	2.6	47.6	4.5	39.5
PTCRSA "whole TW"	5%	11	23	-	-	0.82	11.8	1.47	14.7	47.4	19.4	11.8

References

[1] NAT Doc 007, "Guidance concerning air navigation in and above the North Atlantic MNPS airspace": ICAO, 2012.

[2] Woollings, T., Hannachi, A., and Hoskins, B., "Variability of the North Atlantic eddy-driven jet stream", *Quarterly Journal of the Royal Meteorological Society*, 136, pp. 856–868, 2010.

[3] Mondoloni, S., "Aircraft trajectory prediction errors: Including a summary of error sources and data": Technical report, FAA/Eurocontrol, 1998.

[4] Irvine, E.A., Hoskins, B.J., Shine, K.P., Lunnon, R.W., and Froemming, C., "Characterizing North Atlantic weather patterns for climate-optimal aircraft routing", *Meteorological Applications*, vol. 20, pp. 80–93, 2013.

[5] Office of Aviation Enforcement and Aviation Consumer Protection Division Proceedings: Air Travel Consumer Report, U.S. Department of Transportation, 2015.

[6] Sridhar, B., Sheth, K., Ng, H.K., Morando, A.R. and Li, J., "Global simulation of aviation operations", *AIAA Modeling and Simulation Technologies Conference*, San Diego, CA, USA, 2016.

[7] Chen, N.Y., Kirschen, P.G., Sridhar, B., and Ng, H.K., "Identification of flights for cost-efficient climate impact reduction", *AIAA/3AF Aircraft Noise and Emissions Reduction Symposium*, Atlanta, GA, USA, 2014.

[8] Jardin, M.R., and Bryson, Jr., A.E., "Method for computing minimum-time paths in strong winds", *AIAA Guidance, Navigation, and Control Conference*, Toronto, ON, USA, 2010.

[9] Girardet, B., Lapasset, L., Delahaye, D., and Rabut, C., "Wind-optimal path planning: Application to aircraft trajectories", *13th International Conference on Control, Automation, Robotics and Vision (ICARCV)*, Singapore, Singapore, 2014.

[10] Wickramasinghe, N.K., Harada, A., and Miyazawa, Y., "Flight trajectory optimization for an efficient air transportation system", *28th International Congress of the Aeronautical Science (ICAS)*, Brisbane, Australia, 2012.

[11] Hamy, A., Murrieta-Mendoza, A., and Botez, R., "Flight trajectory optimization to reduce fuel burn and polluting emissions using a performance database and ant colony optimization algorithm", *Advanced Aircraft Efficiency in a Global Air Transport System Conference (AEGATS)*, Paris, France, 2016.

[12] Sridhar, B., Ng, H.K., Linke, F., and Chen, N.Y., "Benefits analysis of wind-optimal operations for trans-Atlantic flights", *14th AIAA Aviation Technology, Integration, and Operations Conference (ATIO)*, Atlanta, GA, USA, 2014.

[13] Ng, H.K., Sridhar, B., Chen, N.Y., and Li, J., "Three-dimensional trajectory design for reducing climate impact of trans-Atlantic flights", *14th AIAA Aviation Technology, Integration, and Operations Conference (ATIO)*, Atlanta, GA, USA, 2014.

[14] Sridhar, B., Ng, H.K., Linke, F., and Chen, N.Y., "Impact of airspace charges on transatlantic aircraft trajectories", *15th AIAA Aviation Technology, Integration, and Operations Conference (ATIO)*, Dallas, TX, USA, 2015.

[15] Doc4444, Air Traffic Management. International Civil Aviation Organization, 15th edition, 2007.

[16] Richards, W.R., O'Brien, K., and Miller, D.C., "New air traffic surveillance technology", *Boeing Aero Quarterly*, vol. 2, 2010.

[17] Automatic Dependent Surveillance - Broadcast In-Trail Procedures (ADS-B ITP) operational flight evaluation: Economic benefits analysis, FAA Surveillance and Broadcast Services Report, 2015.

[18] Gerhardt-Falk, C.M., Elsayed, E.A., Livingston, D., and Colamosca, B., "Simulation of the North Atlantic air traffic and separation scenarios", Technical report, U.S. Department of Transportation, FAA, 2000.

[19] Williams, A., and Greenfeld, I., "Benefits assessment of reduced separations in North Atlantic Organized Track System", *6th AIAA Aviation, Technology, Integration, and Operations Conference (ATIO)*, Wichita, KS, USA, 2006.
[20] Rodionova, O., Sbihi, M., Delahaye, D., and Mongeau, M., "North Atlantic aircraft trajectory optimization", *IEEE Transactions on Intelligent Transportation Systems*, vol. 15(5), pp. 2202–2212, 2014.
[21] Draft Implementation Plan for the Trial Application of RLatSM in the NAT Region, Technical report, European and North Atlantic (EUR/NAT) Office, 2013.
[22] Launius, M., Stehling, K., and Edison, J., "Regional review: North America & North Atlantic regional review", *NBAA International Operators Conference*, San Diego, CA, USA, 2016.
[23] Sridhar, B., Chen, N.Y., Ng, H.K., Rodionova, O., Delahaye, D., and Linke, F., "Strategic planning of efficient oceanic flights", *11th USA/Europe ATM Research and Development Seminar*, Lisbon, Portugal, 2015.
[24] Rodionova, O., Delahaye, D., Sridhar, B., and Ng, H.K., "Deconflicting wind-optimal aircraft trajectories in North Atlantic oceanic airspace", *Advanced Aircraft Efficiency in a Global Air Transport System Conference (AEGATS)*, Paris, France, 2016.
[25] Kuchar, J.K., and Yang, L.C., "A review of conflict detection and resolution modeling methods", *IEEE Transactions on Intelligent Transportation Systems*, vol. 1(4), pp. 179–189, 2000.
[26] Menon, P.K., Sweriduk, G.D., and Sridhar, B., "Optimal strategies for free-flight air traffic conflict resolution", *Journal of Guidance, Control, and Dynamics*, vol. 22(2), pp. 202-210, 1999.
[27] Pallottino, L., Feron, E., and Bucchi, A., "Conflict resolution problem for air traffic management systems solved with mixed integer programming", *IEEE Transactions on Intelligent Transportation Systems*, vol. 3(1), pp. 3–11, 2002.
[28] Christodoulou, M.A., and Kodaxakis, S.G., "Automatic commercial aircraft collision avoidance in free flight: The three-dimensional problem", *IEEE Transactions on Intelligent Transportation Systems*, vol. 7(2), pp. 242–249, 2006.
[29] Dougui, N., Delahaye, D., Peuchmorel, S., and Mongeau, M., "A light propagation model for aircraft trajectory planning", *Journal of Global Optimization*, vol. 56(3), pp. 873–895, 2013.
[30] Mao, Z.H., Feron, E., and Bilimoria, K., "Stability and performance of intersecting aircraft flows under decentralized conflict avoidance rules", *IEEE Transactions on Intelligent Transportation Systems*, vol. 2(2), pp. 101–109, 2001.
[31] Delahaye, D., Peyronne, C., Mongeau, M., and Peuchmorel, S., "Aircraft conflict resolution by genetic algorithm and B-spline approximation", *2nd ENRI International Workshop on ATM/CNS*, pp. 71–78, 2011.
[32] Jardin, M.R., "Real-time conflict-free trajectory optimization", *5th USA/Europe ATM Research and Development Seminar*, Budapest, Hungary, 2003.
[33] Grabbe, S., Sridhar, B., and Mukherjee, A., "Scheduling wind-optimal Central East Pacific flights", *Air Traffic Control Quarterly*, vol. 16(3), pp. 187–210, 2008.
[34] Girardet, B., "Trafic aerien: determination optimale et globale des trajectoires d'avion en presence de vent 'Air traffic: optimal and global determination of aircraft trajectories in the presence of wind'," (in French): PhD thesis, General Mathematics, Toulouse INSA, 2014.
[35] Chaimatanan, S., Delahaye, D., and Mongeau, M., "A hybrid metaheuristic optimization algorithm for strategic planning of 4D aircraft trajectories at the continental scale", *IEEE Computational Intelligence Magazine*, vol. 9(4), pp. 46–61, 2014.
[36] Rodionova, O., "Aircraft trajectory optimization in North Atlantic oceanic airspace": PhD thesis, Toulouse University lll Paul Sabatier, 2015.
[37] Kirkpatrick, S., Gelatt, C.D., and Vecchi, M.P.G., "Optimization by Simulated Annealing", *Science*, vol. 220, pp. 671–680, 1983.
[38] Lee, A.G., Weygandt, S.S., Schwartz, B., and Murphy, J.R., "Performance of trajectory models with wind uncertainties", *AIAA Modeling and Simulation Technologies Conference*, Chicago, IL, USA, 2009.

[39] Tino, C.P., Ren, L., and Clarke, J.-P.B., "Wind forecast error and trajectory prediction for en-route scheduling", *AIAA Guidance, Navigation, and Control Conference*, Chicago, IL, USA, 2009.
[40] Robert, E., and De Smedt, D., "Comparison of operational wind forecasts with recorded flight data", *10th USA/Europe ATM Research and Development Seminar*, Chicago, IL, USA, 2013.
[41] Rodionova, O., Sridhar, B., and Ng, H.K., "Conflict resolution for wind-optimal aircraft trajectories in North Atlantic oceanic airspace with wind uncertainties", *35th Digital Avionics Systems Conference (DASC)*, Sacramento, CA, USA, 2016.
[42] Liang, M., Delahaye, D., and Xu, X.-H., "A novel approach to automated merge 4D arrival trajectories for multi-parallel runways", *4th ENRI International Workshop on ATM/CNS (EIWAC)*, Tokyo, Japan, 2015.